Physiologia Plantarum

ORIGINAL RESEARCH OPEN ACCESS

Divergent Biochemical Strategies and Organ-Specific Metabolic Adjustments in Spinach Mediated by Exogenous Amino Acids Under Salt Stress

Nezahat Turfan[1] | Kübra Tekşen[1] | Ergin Murat Altuner[1] | Faruk Yıldız[2] | Ozkan Kaya[3,4]

[1]Faculty of Science, Department of Biology, Kastamonu University, Kastamonu, Türkiye | [2]Institute of Science, Erzincan Binali Yıldırım University, Erzincan, Türkiye | [3]Erzincan Horticultural Research Institute, Republic of Türkiye Ministry of Agriculture and Forestry, Erzincan, Türkiye | [4]Department of Life Sciences, Western Caspian University, Baku, Azerbaijan

Correspondence: Ozkan Kaya (ozkan.kaya@wcu.edu.az; kayaozkan25@hotmail.com)

Received: 13 November 2025 | **Revised:** 22 February 2026 | **Accepted:** 2 March 2026

Handling Editor: P. Carillo

Keywords: asparagine | ionic homeostasis | phenylalanine | salt stress | secondary metabolism | tryptophan

ABSTRACT

Understanding the physiological and biochemical responses of spinach to salt stress through amino acid supplementation is crucial for improving crop resilience under increasing soil salinity conditions. Salt stress represents one of the most severe abiotic constraints limiting vegetable crop productivity worldwide, yet comprehensive studies examining organ-specific metabolic reprogramming across entire plant systems remain limited. However, knowledge about how different amino acids mediate these responses through distinct metabolic pathways is limited. We investigated mineral nutrition, antioxidant defense systems, and secondary metabolite profiles of spinach supplemented with three amino acids (asparagine, phenylalanine, and tryptophan) under salt stress conditions. Amino acid type, salt treatment, and organ significantly influenced all measured parameters ($p \leq 0.0001$). Asparagine consistently demonstrated comprehensive protective effects, excluding toxic ions while promoting calcium uptake, maintaining photosynthetic capacity, and dramatically enhancing flavonol biosynthesis (quercetin and rutin accumulation increased several-fold) under combined stress compared to other treatments. Phenylalanine excelled in ionic homeostasis restoration, achieving superior Na/K ratio reduction and enhanced phenylpropanoid pathway activation through elevated cinnamic acid biosynthesis. Tryptophan uniquely triggered exceptional divalent cation accumulation (6–10-fold increases in magnesium, calcium, and phosphorus) and maximally enhanced antioxidant enzyme activities, though with notable protein synthesis trade-offs. Organ-specific accumulation patterns revealed leaves as primary sites for photosynthetic pigments and phenolic compounds, roots as storage organs for specialized flavonoids and catechins, and petioles showing exceptional rutin accumulation. These findings demonstrate that amino acid selection fundamentally reshapes metabolic priorities in salt-stressed spinach through divergent yet complementary biochemical strategies. We conclude that amino acid selection significantly influences spinach resilience to salt stress through divergent metabolic reprogramming strategies, with each amino acid offering distinct advantages depending on cultivation priorities. Differential metabolic responses between amino acids provide insights for precision agriculture applications, while the quantitative biochemical patterns identified offer valuable parameters for optimizing amino acid supplementation strategies under saline conditions.

1 | Introduction

Spinach (*Spinacia oleracea*), a prominent member of the Amaranthaceae family, stands as one of the most widely cultivated dark leafy green vegetables worldwide, encompassing winter cultivars that exhibit significant cold tolerance, and summer cultivars characterized by shorter vegetative phases suited for rapid cultivation (Turfan et al. 2024). This versatile crop distinguishes itself through its exceptional nutritional profile, featuring high contents of dietary fiber, lutein, beta-carotene, vitamins, phenolic compounds, and flavonoids alongside remarkably low caloric content, collectively positioning spinach among the most effective vegetables for preventing obesity, hypertension, cardiovascular diseases, and gastrointestinal disorders (Chouaibi 2025). Moreover, the Centers for Disease Control and Prevention (CDC) ranks spinach among the top five most nutrient-dense vegetables, attributable to its richness in essential minerals such as iron, calcium, magnesium, and potassium, as well as vitamins A, C, E, and K (Kim et al. 2021). The ability to cultivate spinach throughout all seasons, coupled with relatively low input requirements and year-round market availability, has contributed to its widespread cultivation across diverse global regions, with production reaching approximately 30.8 million tons in 2024, of which China accounts for about 92%, while Türkiye ranks third with approximately 237,000 tons (FAO 2024; TURKSTAT 2024).

Beyond its nutritional significance, spinach represents a particularly suitable crop for reclaiming saline-affected areas due to its moderate salt tolerance and broad ecological plasticity, where moderately salt-tolerant crops offer distinct advantages by reducing research costs and enhancing resilience to environmental stresses. However, despite demonstrating moderate tolerance to salinity, spinach cultivation is becoming progressively more vulnerable to soil deterioration and climate-related abiotic stresses (Turfan et al. 2024). Salinity, escalated by improper irrigation, excessive fertilization, and intensive use of pesticides and herbicides, leads to the accumulation of soluble salts in the soil, causing significant yield losses. Furthermore, as the global population continues to grow, having already surpassed 8.2 billion in recent years (El-Awadi et al. 2025), soil salinization presents an escalating threat to food security, where according to the Food and Agriculture Organization (FAO 2024), nearly 750 million people suffer from hunger and malnutrition, with this figure expected to rise unless sustainable agricultural practices are adopted. The detrimental effects of salt stress on spinach are multifaceted and interconnected, where salt stress primarily induces ion toxicity, subsequently triggering osmotic imbalance and oxidative stress (Khattab et al. 2024). The excessive accumulation of Na and Cl suppresses mitotic activity, thereby inhibiting root development while simultaneously restricting water and nutrient uptake (Yin et al. 2023; El-Lethy et al. 2024). Concurrently, salt-induced oxidative stress exacerbates cellular damage via lipid peroxidation and impairs photosynthetic efficiency, culminating in inhibited growth, reduced biomass accumulation, and compromised crop productivity (Hussain et al. 2018; Sadak et al. 2024). These multifaceted detrimental effects necessitate innovative approaches to enhance plant resilience, making the strategic development of salt-tolerant cultivars alongside resilient agronomic practices vital to ensure food security and maintain ecosystem stability.

In this context, biostimulants such as amino acids present promising strategies to enhance plant resilience under saline conditions. Amino acids, when applied through foliar sprays, can rapidly diffuse through stomata and directly engage in protein synthesis, ATP production, and metabolic regulation (Sadak et al. 2015; Zhang et al. 2017). Moreover, these compounds serve as nitrogen sources by forming N-containing molecules such as pigments, secondary metabolites, and osmolytes, thereby supporting nitrogen balance and promoting vegetative growth and yield, while also enhancing antioxidant defenses that alleviate salt-induced physiological and anatomical damage (Sadak et al. 2015; Akın and Kaya 2024). The choice of amino acid is particularly important because structurally different amino acids enter distinct metabolic pathways: asparagine (ASN) functions primarily as a nitrogen donor and storage compound involved in nitrogen redistribution (Guo et al. 2023); phenylalanine (PHE) serves as the direct precursor of the phenylpropanoid pathway via phenylalanine ammonia-lyase (PAL) activity, channeling carbon flux into phenolic compound biosynthesis (Feduraev et al. 2020); and tryptophan (TRP) acts as a precursor for auxin biosynthesis and indole-derived secondary metabolites including glucosinolates and alkaloids (Jamil et al. 2018; Turfan et al. 2024). Despite these distinct metabolic roles, comparative studies examining how these three amino acids differentially modulate the complete biochemical response of spinach to salt stress across multiple organs have not been conducted. Recent studies have increasingly concentrated on foliar supplementation with amino acids, including asparagine (ASN) (Akın and Kaya 2024), phenylalanine (PHE) (Almas et al. 2021; Sadak et al. 2025), tryptophan (TRP) (Turfan et al. 2024), tyrosine (Turfan 2023), glycine betaine (Khan et al. 2018), and proline (Jamil et al. 2018), as effective approaches to mitigate salinity-induced damage and improve plant stress tolerance. These compounds accelerate the biosynthesis of proteins, enzymes, hormones, and pigments that contribute to plant growth, enhance carbon fixation, and improve biomass accumulation, thereby optimizing yield (Bakhoum et al. 2019; Atteya et al. 2022). As bioinducers, amino acids also stimulate cell division, improve mineral absorption and utilization efficiency, and foster favorable conditions for root development by regulating soil microorganisms (Marium et al. 2021). Previous studies have demonstrated that foliar application of amino acids promotes vegetative growth, including increases in leaf, shoot, and root biomass, by inducing metabolite accumulation (Almas et al. 2021) and enhancing antioxidant metabolism, thereby improving both yield and quality (Atteya et al. 2022).

Despite the growing body of research, comprehensive studies examining the effects of salinity across the entire spinach plant, particularly integrating leaves, petioles, and roots, remain limited. This knowledge gap is particularly significant considering that photo assimilates produced in the leaves are transported to other organs via the petioles, making it important to understand how salt stress affects this transport process (Liu et al. 2023). In Türkiye, where research on this issue remains limited, addressing this knowledge gap becomes increasingly important for advancing sustainable spinach production under saline conditions. From this perspective, this study aims to examine the effects of salt stress on spinach's leaves, petioles, and roots, while exploring how external stimulants may modulate these responses. We hypothesize that foliar supplementation with asparagine (ASN),

phenylalanine (PHE), and tryptophan (TRP) during the early growth stages could enhance both growth and resilience to salt stress in spinach. Therefore, the objectives of this study are: (I) to investigate the impact of foliar applications of ASN, PHE, and TRP on various growth parameters under saline conditions, (II) to evaluate their effects on biochemical composition, antioxidant activity, and oxidative stress markers, and (III) to determine the underlying mechanisms by which these amino acids confer salt stress tolerance in spinach for improved sustainable production, with particular emphasis on organ-specific metabolic specialization and the differential biochemical strategies employed by each amino acid.

2 | Materials and Methods

2.1 | Plant Material and Chemicals

Spinach seeds (*Spinacia oleracea* L. cv. Efsun F1) were obtained from the MAY Seed Company. Sodium chloride (NaCl, CAS: 7647-14-5), L-asparagine (CAS: 5794-13-8), L-phenylalanine (CAS: 63-91-2), and L-tryptophan (CAS: 73-22-3) were purchased from Merck.

2.2 | Determination of Effective Doses

The optimal concentrations of NaCl, L-ASN, L-PHE, and L-TRP were determined through preliminary germination experiments (Turfan et al. 2024; Turfan 2025; Table 1). NaCl solutions were prepared at concentrations of 50, 100, 200, and 250 mM, corresponding to electrical conductivity (EC) values of approximately 5.0, 10.0, 20.0, and 25.0 dS m^{-1}, respectively. Similarly, aqueous solutions of ASN, PHE, and TRP were prepared at concentrations ranging from 1.2 to 8.2 mM. Sterilized seeds were soaked in these solutions for 4 h before being placed in petri dishes containing filter paper. The salt concentration that reduced germination by more than 60% compared to control (~28–32 seeds) was selected as the stress level, while for amino acids, the concentration yielding more than 60% germination success (~48–50 seeds) was chosen as the optimal dose. Based on these criteria, final concentrations were established at 250 mM NaCl, 2.4 mM L-ASN, 4.6 mM L-PHE, and 3.6 mM L-TRP.

2.3 | Experimental Design and Growth Conditions

Spinach seedlings were grown in a controlled growth chamber maintained at 18°C ± 1°C with 50%–65% relative humidity under a 12 h light/12 h dark photoperiod at a light intensity of 150 μmol m^{-2} s^{-1} provided by fluorescent lamps. The experiment was arranged as a completely randomized design using seedling trays (12 × 12 × 10 cm) with 16 wells per tray. Each well was filled with a peat: perlite mixture (3:1) as the growing medium. Seeds were sown at a density of 3-4 seeds per well in November 2024, with immediate irrigation following sowing. Seedlings were thinned to one plant per well 15 days after sowing. Treatment applications commenced when seedlings developed 5-6 leaves. Eight treatment groups were established: Control, NaCl, ASN, ASN-NaCl, PHE, PHE-NaCl, TRP, and TRP-NaCl (Table 1). Treatments were applied twice weekly for 6 weeks. Salt treatments were administered via soil irrigation (10–15 mL per plant), while amino acid applications were applied as foliar sprays (10–12 mL per plant), ensuring complete coverage of both adaxial and abaxial leaf surfaces. Control plants received foliar applications with water. Throughout the experiment, irrigation was maintained uniformly across all treatments. Plants were harvested in March 2025 by carefully removing entire seedlings with intact root systems from the growing medium.

2.4 | Biochemical Analyses

2.4.1 | Mineral Analysis

Mineral content (P, K, Ca, Mg, Na, Cl, and S) in leaves and roots was analyzed following oven-drying at 65°C for 48 h. Dried samples were ground using a laboratory grinder (MC23200, Siemens) and subjected to microwave-assisted acid digestion. Elemental analysis was performed using X-ray fluorescence spectrometry (Spectro XEPOS) at the Central Research Laboratory of Kastamonu University.

2.4.2 | Antioxidant Capacity Assays

Ferric reducing antioxidant power (FRAP) was determined following Benzie and Strain (1996). Extracts (500 μg mL^{-1}) were combined with FRAP reagent and incubated in darkness for 20 min at room temperature. Absorbance was measured at 700 nm, with ascorbic acid as the positive control. Results were expressed as μg ascorbic acid equivalents per mg fresh weight. Total antioxidant capacity was determined using the phosphomolybdenum method described by Prieto et al. (1999), which is based on the reduction of Mo(VI) to Mo(V) by the sample, forming a green phosphate/Mo(V) complex under acidic conditions. Briefly, 0.1 mL of sample extract was combined with 0.3 mL of reagent solution containing 0.6 M sulfuric acid, 28 mM sodium phosphate, and 4 mM ammonium molybdate. The mixture was incubated at 95°C for 90 min, cooled to room temperature, and absorbance was measured at 695 nm against a reagent blank. Total antioxidant capacity was then calculated according to the following equation:

$$\text{Total antioxidant capacity}\,(\%) = \left[(\text{A695 Control} - \text{A695 Sample}) / (\text{A695 Control})\right] \times 100$$

Superoxide dismutase (SOD), catalase (CAT), and ascorbate peroxidase (APX) activities were determined in fresh leaf and root tissues. Samples (0.5 g) were homogenized in ice-cold 50 mM potassium phosphate buffer (pH 7.0) containing 1 mM EDTA and centrifuged at 12,000 × *g* for 20 min at 4°C. The supernatant was used for enzyme assays. SOD activity was measured based on the inhibition of nitroblue tetrazolium (NBT) photoreduction at 560 nm according to Beauchamp and Fridovich (1971). One unit of SOD activity was defined as the amount of enzyme causing 50% inhibition of NBT reduction. CAT activity was determined by monitoring the decomposition of H_2O_2 at 240 nm following the method of Aebi (1984). Enzyme activity was calculated using the extinction coefficient of H_2O_2 and expressed as U mg^{-1} protein. APX activity was assayed by measuring the decrease in absorbance at 290 nm due to ascorbate oxidation in the presence of

TABLE 1 | Mineral nutrient concentrations and ionic ratios in leaf, petiole, and root tissues of spinach plants under different amino acid and biostimulant treatment combinations.

Applications		Na (mg kg^{-1})	Cl (mg kg^{-1})	Mg (mg kg^{-1})	Ca (mg kg^{-1})	K (mg kg^{-1})	P (mg kg^{-1})	S (mg kg^{-1})	Na/Cl	Na/K
Treatment	Control	16523.0 ± 356.5^{b}	18925.4 ± 487.0^{c}	5085.1 ± 657.6^{b}	4319.4 ± 149.4^{f}	28595.8 ± 692.9^{b}	1478.9 ± 177.0^{e}	692.8 ± 411.0^{c}	0.90 ± 0.00^{a}	0.58 ± 0.01^{c}
	NaCl	63690.9 ± 9569.1^{a}	72051.1 ± 9569.2^{a}	4175.7 ± 267.5^{b}	4235.6 ± 116.7^{g}	32229.4 ± 692.9^{a}	1791.6 ± 129.5^{b}	691.6 ± 244.0^{c}	0.89 ± 0.00^{b}	2.01 ± 0.34^{a}
	ASN	14446.3 ± 777.6^{d}	17814.7 ± 709.0^{f}	4302.2 ± 118.6^{b}	7372.1 ± 117.1^{b}	19753.4 ± 753.4^{e}	1379.8 ± 980.6^{f}	584.6 ± 556.6^{e}	0.81 ± 0.00^{c}	0.76 ± 0.01^{b}
	PHE	7208.9 ± 849.6^{h}	11284.8 ± 669.0^{g}	4716.3 ± 236.4^{b}	5575.0 ± 988.5^{e}	26692.7 ± 692.9^{c}	1570.6 ± 778.1^{d}	708.1 ± 512.1^{b}	0.64 ± 0.00^{e}	0.28 ± 0.00^{d}
	TRP	7661.3 ± 778.0^{g}	9763.0 ± 129.1^{h}	3848.4 ± 145.7^{b}	5723.2 ± 45.6^{d}	25442.8 ± 692.9^{c}	1780.7 ± 878.6^{b}	707.7 ± 753.0^{b}	0.78 ± 0.00^{d}	0.31 ± 0.01^{d}
	ASN + NaCl	12099.1 ± 651.6^{f}	25446.4 ± 755.0^{d}	4154.8 ± 843.5^{b}	7374.8 ± 157.2^{b}	18980.6 ± 980.6^{e}	1313.1 ± 788.1^{g}	626.0 ± 756.2^{d}	0.48 ± 0.00^{g}	0.63 ± 0.01^{c}
	PHE + NaCl	13083.3 ± 409.6^{e}	27303.7 ± 457.1^{c}	4422.8 ± 217.9^{b}	6982.2 ± 20.2^{c}	23363.4 ± 363.4^{d}	1652.6 ± 137.1^{e}	794.9 ± 458.0^{a}	0.48 ± 0.00^{f}	0.57 ± 0.00^{c}
	TRP + NaCl	14995.4 ± 998.2^{c}	30746.6 ± 948.6^{b}	40414.3 ± 664.7^{a}	44743.9 ± 39.7^{a}	18836.2 ± 836.2^{e}	15088.0 ± 598.7^{a}	587.1 ± 623.6^{e}	0.48 ± 0.00^{fg}	0.78 ± 0.00^{b}
Organ	Leaf	20585.8 ± 52.1^{a}	30932.3 ± 3.5^{a}	10631.0 ± 462.5^{a}	11955.8 ± 5.1^{a}	26550.1 ± 215.3^{a}	3609.6 ± 3.4^{a}	893.5 ± 1.2^{a}	0.63 ± 0.01^{c}	0.75 ± 0.01^{b}
	Petiole	17142.1 ± 34.1^{c}	25261.9 ± 3.5^{b}	8150.0 ± 462.5^{b}	10052.5 ± 5.1^{c}	24972.5 ± 215.3^{b}	2916.0 ± 3.4^{c}	605.6 ± 1.2^{b}	0.67 ± 0.01^{b}	0.66 ± 0.01^{c}
	Root	18412.7 ± 45.1^{b}	23806.7 ± 3.5^{c}	7888.8 ± 462.5^{b}	10364.0 ± 5.1^{b}	21187.8 ± 215.3^{c}	3245.1 ± 3.4^{b}	523.1 ± 1.2^{c}	0.75 ± 0.01^{a}	0.81 ± 0.01^{a}
Treatment	*p* value	< 0.0001	< 0.0001	< 0.0001	< 0.0001	< 0.0001	< 0.0001	< 0.0001	< 0.0001	< 0.0001
Organ	*p* value	< 0.0001	< 0.0001	< 0.0002	< 0.0001	< 0.0001	< 0.0001	< 0.0001	< 0.0001	< 0.0002
T × O	*p* value	< 0.0001	< 0.0001	< 0.0001	< 0.0001	< 0.0002	< 0.0001	< 0.0001	< 0.0001	< 0.0001

Note: Values are means ± standard error ($n = 3$). Different superscript letters within each column indicate significant differences among treatment × organ combinations according to Tukey's HSD test. Statistical significance was determined at $p < 0.0001$ for treatment, organ, and treatment × organ interaction (T × O) effects.

H_2O_2 according to Nakano and Asada (1981). Enzyme activity was calculated using the extinction coefficient of ascorbate and expressed as U mg^{-1} FW.

2.4.3 | Protein Content

Total protein content in leaf and root tissues was determined using the Kjeldahl method (Bradstreet 1954). Briefly, oven-dried samples were digested with concentrated H_2SO_4 in the presence of a catalyst mixture until a clear solution was obtained. The digested samples were then subjected to alkaline distillation, and the released ammonia was trapped in boric acid solution and titrated with standardized HCl. Total nitrogen content was calculated, and crude protein content was estimated using a conversion factor of 6.25. Results were expressed as % dry weight.

2.4.4 | Chlorophyll and Carotenoid Content

Photosynthetic pigments were extracted from fresh leaf tissue (0.2 g) using 80% acetone and centrifuged at 10,000 × *g* for 10 min. The absorbance of the supernatant was recorded at 663, 645, and 470 nm using a UV–visible spectrophotometer. Total chlorophyll and carotenoid contents were calculated according to Lichtenthaler (1987) and expressed as mg g^{-1} fresh weight.

2.4.5 | Anthocyanin Content

Anthocyanin (ANT) content was quantified following Mancinelli (1990). Briefly, 500 mg of fresh tissue was extracted with 3 mL of 1% HCl-acidified methanol and stored at 4°C for 48 h with intermittent agitation. After filtration, absorbance was measured at 530 nm. ANT concentration was calculated using an extinction coefficient of 31.6 M^{-1} cm^{-1}.

2.4.6 | Ascorbic Acid and Proline Content

Ascorbic acid (AsA) content was determined according to Kumaran and Karunakaran (2006). Fresh tissue was homogenized in cold extraction buffer, centrifuged, and the absorbance of the supernatant was measured spectrophotometrically at the specified wavelength. Results were expressed as mg g^{-1} fresh weight. Free proline content was measured following Bates et al. (1973). Fresh tissue was extracted with 3% sulfosalicylic acid and reacted with acid ninhydrin reagent. The reaction mixture was incubated at 100°C for 1 h, terminated in an ice bath, and extracted with 4 mL of toluene. The absorbance of the chromophore-containing toluene phase was measured at 520 nm using a UV–visible spectrophotometer (Unico S2100). Proline concentrations were calculated from a standard curve and expressed as μmol g^{-1} fresh weight.

2.4.7 | Total Phenolic and Flavonoid Content

Total phenolic content (TPC) was determined using the Folin-Ciocalteu method (Singleton and Rossi 1965). A 500 μL aliquot of methanolic extract was mixed with Folin-Ciocalteu reagent and sodium carbonate, then incubated for 2 h. Absorbance was measured at 765 nm, and TPC was expressed as mg gallic acid equivalents (GAE) per gram dry weight using a standard curve ($R^2 = 0.994$). Total flavonoid content (TFC) was assessed according to Kumaran and Karunakaran (2006). Extract (100 μL) was combined with 100 μL of 20% $AlCl_2$, adjusted to 5 mL, and incubated for 40 min at room temperature. Absorbance was measured at 415 nm, and TFC was calculated using a quercetin standard curve ($R^2 = 0.994$).

2.4.8 | Phenolic Acid Analysis

Phenolic acid composition was analyzed using HPLC-MS/MS following Rodrıguez-Delgado et al. (2001). Fresh tissue (10 g) was crushed, centrifuged at 10,000 × *g* for 15 min at 4°C, and filtered. A 10 μL aliquot was injected into an Agilent HPLC system equipped with an ODS4 column. The mobile phase consisted of methanol, acetic acid, and water at a flow rate of 1 mL min^{-1}. UV absorbance was recorded at 254 and 280 nm. Calibration standards were prepared in methanol at concentrations ranging from 0.0312 to 1.0000 mg L^{-1}.

2.5 | Statistical Analysis

Data were analyzed using multivariate analysis of variance (MANOVA), followed by Tukey's Honestly Significant Difference (HSD) test ($p < 0.05$) for post hoc comparisons. Statistical analyses were conducted using R Studio. Principal component analysis (PCA) was performed to visualize relationships among variables and observations in reduced-dimensional space.

3 | Results

3.1 | Amino Acid Effects on Mineral Nutrition and Ionic Balance in Salt-Stressed Spinach

Mineral nutrient analysis of spinach tissues revealed significant treatment, organ, and treatment × organ interaction effects ($p < 0.0001$) across all measured parameters (Table 1 and Figure 1). Sodium and chloride accumulation were most pronounced under NaCl stress, with treatment averages reaching 63690.9 and 72051.1 mg kg^{-1}, respectively, while leaves exhibited peak Na^+ (68861.3 mg kg^{-1}) and roots showed maximum Cl^- (77255.7 mg kg^{-1}) concentrations. Amino acid supplementation effectively mitigated ionic toxicity, with asparagine reducing leaf Na^+ by 76% in ASN + NaCl treatment (16346.0 mg kg^{-1}) compared to NaCl alone. Phenylalanine demonstrated superior protective effects, maintaining the lowest Na treatment average (7208.9 mg kg^{-1}), while both PHE and TRP treatments exhibited exceptional chloride exclusion capacity (11284.8 and 9763.0 mg kg^{-1}, respectively). From an organ distribution perspective, leaves accumulated the highest average Na (20585.8 mg kg^{-1}) and Cl (30932.3 mg kg^{-1}), followed by roots and petioles, though amino acid applications substantially reduced these concentrations across all tissues. A remarkable finding was the exceptional accumulation of magnesium, calcium, and phosphorus in TRP + NaCl-treated plants, with treatment averages

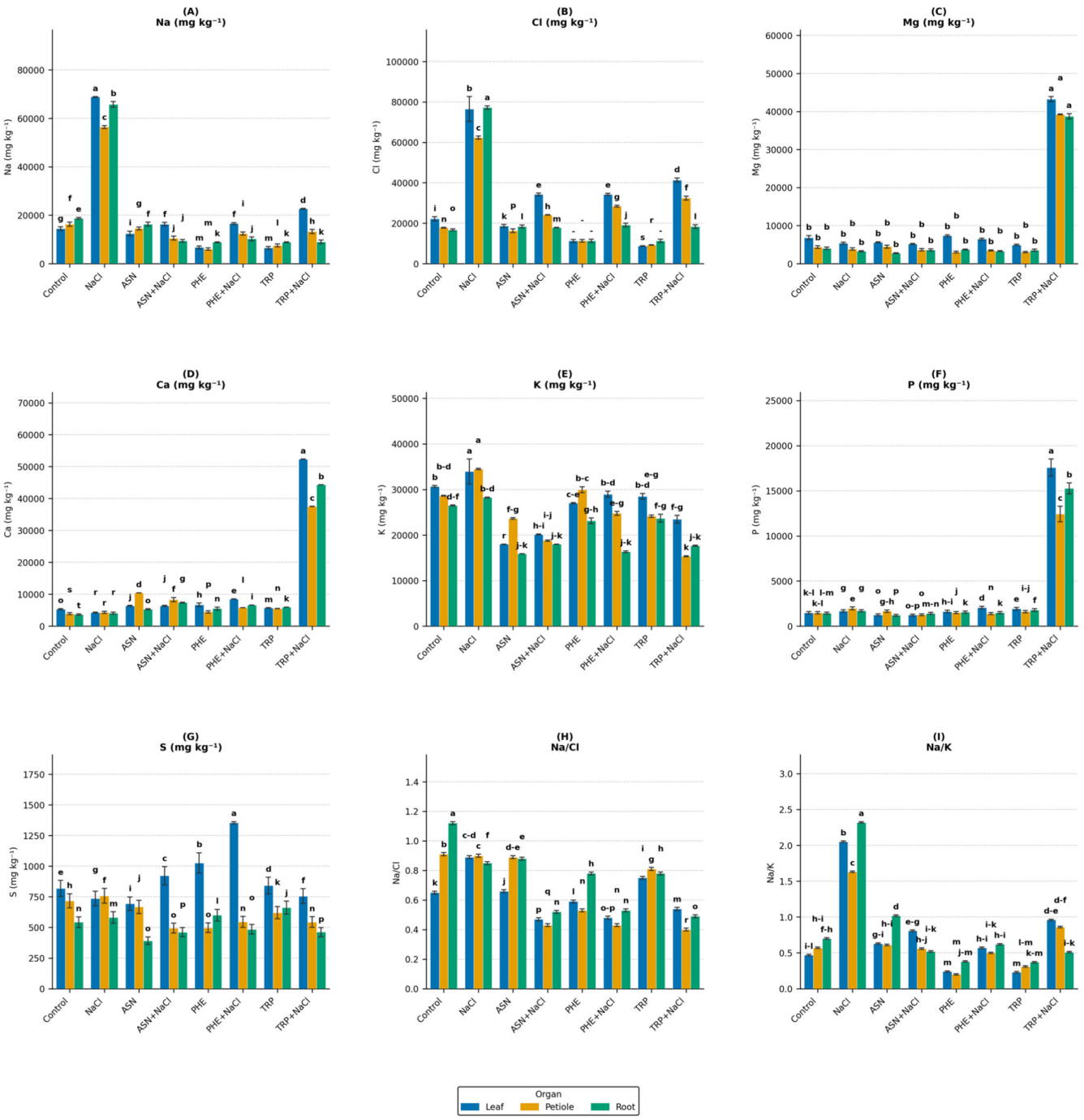

FIGURE 1 | Mineral nutrient concentrations and ionic ratios in leaf, petiole, and root tissues of spinach (*Spinacia oleracea* L.) plants subjected to exogenous amino acid and biostimulant applications under salt stress conditions. Values are means ± SE ($n = 3$). Different lowercase letters above bars indicate significant differences among treatment × organ combinations (Tukey's HSD test, $p < 0.0001$ for treatment, organ, and treatment × organ interaction effects).

of 40414.3, 44743.9, and 15088.0 mg kg^{-1}, respectively, representing 6–10 fold increases compared to control plants (5085.1, 4319.4, and 1478.9 mg kg^{-1}). Within TRP + NaCl treatment, leaves showed the highest concentrations for all three nutrients, with Mg reaching 43244.3 mg kg^{-1}, Ca 52346.0 mg kg^{-1}, and P 17563.7 mg kg^{-1}. This coordinated elevation suggests tryptophan triggers a unique divalent cation and phosphate uptake mechanism under salinity, potentially through enhanced root metabolic activity or altered membrane transporter expression. Asparagine also enhanced Ca uptake (treatment average: 7372.1 mg kg^{-1}), with petioles showing remarkable accumulation (10436.3 mg kg^{-1}), while NaCl stress alone resulted in the lowest Ca concentrations (4235.6 mg kg^{-1}), indicating salt-induced Ca^{2+} deficiency.

Potassium nutrition showed contrasting patterns, with NaCl stress inducing the highest K^+ accumulation (32229.4 mg kg^{-1}), suggesting compensatory uptake mechanisms. However,

amino acid treatments substantially reduced K levels, with ASN + NaCl showing the lowest treatment average (18980.6 mg kg^{-1}), indicating potential K^+-amino acid antagonism. This inverse relationship between amino acid supplementation and K^+ levels, contrasting with enhanced Ca^{2+} and Mg^{2+} uptake, suggests amino acids modulate cation-specific transport systems, prioritizing divalent over monovalent cation acquisition under both optimal and stress conditions. Leaves maintained the highest average K (26550 mg kg^{-1}), demonstrating preferential K^+ allocation to photosynthetic tissues. Sulfur concentrations were highest in PHE + NaCl treatment (794.9 mg kg^{-1}), with leaves showing exceptional accumulation (1354.7 mg kg^{-1}), a 66% increase compared to control leaves (818.0 mg kg^{-1}). This PHE + NaCl-specific enhancement suggests phenylalanine promotes sulfate uptake and assimilation under salinity, potentially supporting synthesis of sulfur-containing antioxidants such as glutathione and phytochelatins. In contrast, asparagine treatments resulted in the lowest S levels (ASN: 584.6 mg kg^{-1}; ASN + NaCl: 626.0 mg kg^{-1}). The Na/K ratio, a critical indicator of salt stress severity, increased 3.5-fold under NaCl stress (2.01) compared to control (0.58), with roots exhibiting the highest value (2.32), indicating severe disruption of K^+/Na^+ selectivity. Remarkably, all amino acid treatments under salinity effectively restored ionic balance: ASN + NaCl (0.63), PHE + NaCl (0.57), and TRP + NaCl (0.78) maintained ratios comparable to control levels. Phenylalanine demonstrated superior performance, achieving a 72% reduction in Na/K ratio compared to NaCl alone. The Na/Cl ratio was consistently 0.48 across all amino acid-salinity combinations, representing a 47% reduction compared to control (0.90), indicating amino acids establish a new ionic equilibrium through coordinated regulation of Na^+ and Cl^- transporters. Overall, phenylalanine excelled in maintaining ionic homeostasis with the lowest Na/K ratio and enhanced sulfur nutrition, asparagine effectively excluded toxic ions while promoting calcium uptake, and tryptophan uniquely activated multiple nutrient uptake pathways under salinity, though with notable trade-offs in potassium acquisition (Table 1 and Figure 1).

3.2 | Amino Acid Effects on Antioxidant Defense and Secondary Metabolites in Salt-Stressed Spinach

Antioxidant enzyme activities showed significant treatment, organ, and treatment × organ ($p < 0.0001$) interaction effects across all parameters (Table 2 and Figure 2). Tryptophan treatment induced the highest activities for CAT (63.48 U mg^{-1} FW) and SOD (170.29 U mg^{-1} FW), while phenylalanine equally enhanced APX activity (5.36 U mg^{-1} FW). TRP leaves exhibited maximum activities: APX (6.54 U mg^{-1} FW), CAT (78.17 U mg^{-1} FW), and SOD (188.50 U mg^{-1} FW), representing 23%–50% increases compared to control leaves. NaCl stress alone resulted in the lowest enzyme activities (APX: 3.50; CAT: 35.69; SOD: 93.01 U mg^{-1} FW), indicating impaired antioxidant defense. Under combined stress, TRP + NaCl maintained the highest protection (APX: 4.85; CAT: 50.15; SOD: 156.60 U mg^{-1} FW), representing 36%–68% enhancements compared to NaCl alone. PHE + NaCl and ASN + NaCl also showed substantial improvements across all enzymes. From an organ perspective, leaves consistently exhibited the highest enzyme activities, followed by petioles and roots, reflecting greater antioxidant demand in photosynthetic tissues. Protein content revealed contrasting patterns, with control plants maintaining the highest levels (23.21%), while NaCl stress dramatically reduced protein to 17.64%, particularly in roots (10.84%). A remarkable finding was ASN + NaCl roots exhibiting the highest protein concentration (32.12%), representing a 196% increase compared to NaCl-stressed roots, suggesting asparagine uniquely enhanced protein accumulation in roots under salinity. Conversely, TRP and TRP + NaCl treatments resulted in the lowest protein content (14.16% and 15.65%), indicating metabolic trade-offs where tryptophan's remarkable enhancement of mineral nutrition occurred at the expense of protein synthesis. Leaves maintained the highest average protein (21.8%), followed by roots (20.3%) and petioles (14.4%). Proline, a key osmolyte, accumulated to the highest levels under amino acid-salinity combinations, with TRP + NaCl and ASN + NaCl showing treatment averages of 239.89 and 234.37 μmol g^{-1}, respectively, representing 13%–16% increases compared to control (206.99 μmol g^{-1}). ASN + NaCl leaves exhibited maximum proline concentration (263.25 μmol g^{-1}), followed by TRP + NaCl leaves (260.35 μmol g^{-1}), indicating amino acid-mediated enhancement of osmolyte biosynthesis for osmotic adjustment and protein stability. Leaves showed the highest average proline (240.4 μmol g^{-1}), reflecting preferential accumulation in photosynthetic tissues.

Photosynthetic pigments revealed differential responses to amino acid treatments. Asparagine maintained the highest chlorophyll levels (1.43 mg g^{-1}), with ASN + NaCl effectively protecting against salt-induced degradation (1.40 vs. 1.07 mg g^{-1} in NaCl alone), representing 31% enhancement. TRP + NaCl leaves (2.24 mg g^{-1}) also showed substantial chlorophyll recovery. Carotenoid content was highest in ASN + NaCl treatment (12.06 mg g^{-1}), with TRP and PHE leaves showing maximum concentrations (13.39 and 13.19 mg g^{-1}), representing 22%–28% increases compared to control, suggesting enhanced biosynthesis of photoprotective pigments to mitigate oxidative stress. Secondary metabolite profiles demonstrated pronounced amino acid-specific enhancements. Anthocyanin accumulation was highest in PHE and TRP treatments 0.74 (μmol g^{-1} for both), with TRP + NaCl leaves showing maximum concentration (0.96 μmol g^{-1}), a 71% increase compared to control leaves (0.56 μmol g^{-1}). NaCl stress alone resulted in the lowest anthocyanin content (0.30 μmol g^{-1}), while amino acid supplementation under salinity restored levels substantially. Catechin content showed the most dramatic response, with PHE + NaCl inducing the highest accumulation (15.56 mg g^{-1}), particularly in roots (22.58 mg g^{-1}), representing a 10-fold increase compared to control roots. TRP treatments also substantially enhanced catechin levels (TRP: 13.21; TRP + NaCl: 11.48 mg g^{-1}). Interestingly, roots exhibited the highest average catechin content (11.6 mg g^{-1}), indicating preferential accumulation of these flavonoid antioxidants in below-ground tissues. Overall, aromatic amino acids (PHE and TRP) demonstrated superior performance in activating antioxidant enzyme systems and stimulating phenylpropanoid pathway-derived secondary metabolites, while asparagine excelled in maintaining chlorophyll content, enhancing carotenoid biosynthesis, and uniquely promoting protein accumulation in roots under salinity, suggesting complementary yet distinct mechanisms of stress tolerance enhancement (Table 2 and Figure 2).

TABLE 2 | Effect of exogenous amino acid applications on antioxidant enzyme activities, protein content, osmolytes, and secondary metabolite concentrations in leaf, petiole, and root tissues of spinach plants under salt stress conditions.

Applications		APX (U mg^{-1} FW)	CAT (U mg^{-1} FW)	SOD (U mg^{-1} FW)	Protein (%)	Proline (μmol g^{-1})	Chlorophyll (mg g^{-1})	Carotenoid (mg g^{-1})	Anthocyanin (μmol g^{-1})	Catechin (mg g^{-1})
Treatment	Control	3.68 ± 0.32^{e}	45.86 ± 2.45^{f}	104.88 ± 6.78^{g}	23.21 ± 1.11^{a}	206.99 ± 2.45^{e}	1.19 ± 0.21^{d}	8.60 ± 0.34^{f}	0.41 ± 0.07^{e}	1.03 ± 0.56^{h}
	NaCl	3.50 ± 0.45^{e}	35.69 ± 7.65^{h}	93.01 ± 1.21^{h}	17.64 ± 2.32^{e}	213.75 ± 9.87^{d}	1.07 ± 0.44^{f}	9.04 ± 0.98^{e}	0.30 ± 0.12^{f}	4.66 ± 1.23^{g}
	ASN	4.52 ± 0.33^{c}	52.54 ± 2.11^{c}	119.94 ± 9.87^{e}	20.29 ± 1.23^{c}	218.99 ± 1.45^{c}	1.43 ± 0.32^{a}	11.74 ± 1.21^{b}	0.70 ± 0.02^{b}	5.88 ± 1.21^{f}
	PHE	5.36 ± 1.23^{a}	56.39 ± 4.45^{b}	147.77 ± 11.12^{c}	20.67 ± 0.98^{b}	218.38 ± 6.32^{cd}	1.20 ± 0.45^{d}	8.58 ± 1.88^{f}	0.74 ± 0.12^{a}	12.97 ± 1.45^{c}
	TRP	5.36 ± 1.33^{a}	63.48 ± 8.22^{a}	170.29 ± 6.33^{a}	14.16 ± 3.11^{g}	218.78 ± 4.45^{c}	1.13 ± 0.78^{e}	10.19 ± 1.12^{d}	0.74 ± 0.08^{a}	13.21 ± 1.12^{b}
	ASN + NaCl	4.00 ± 1.22^{d}	46.38 ± 8.12^{e}	108.98 ± 3.11^{f}	20.33 ± 1.98^{c}	234.37 ± 2.11^{b}	1.40 ± 0.44^{b}	12.06 ± 2.87^{a}	0.41 ± 0.03^{e}	8.32 ± 1.22^{e}
	PHE + NaCl	4.77 ± 1.11^{bc}	42.69 ± 3.45^{g}	140.46 ± 1.22^{d}	18.59 ± 0.78^{d}	207.16 ± 4.11^{e}	1.07 ± 0.33^{f}	8.27 ± 2.11^{g}	0.49 ± 0.08^{d}	15.56 ± 1.33^{a}
	TRP + NaCl	4.85 ± 1.11^{b}	50.15 ± 2.87^{d}	156.60 ± 1.33^{b}	15.65 ± 1.12^{f}	239.89 ± 3.45^{a}	1.23 ± 0.33^{c}	10.53 ± 1.12^{c}	0.56 ± 0.01^{c}	11.48 ± 1.78^{d}
Organ	Leaf	5.79 ± 0.0^{a}	60.9 ± 0.5^{a}	147.7 ± 0.0^{a}	21.8 ± 0.0^{a}	240.4 ± 0.6^{a}	2.01 ± 0.02^{a}	12.0 ± 0.3^{a}	0.70 ± 0.01^{a}	5.7 ± 0.2^{c}
	Petiole	4.29 ± 0.0^{b}	48.4 ± 0.5^{b}	131.7 ± 0.7^{b}	14.4 ± 0.0^{c}	211.0 ± 0.6^{b}	1.00 ± 0.01^{b}	10.2 ± 0.0^{b}	0.53 ± 0.00^{b}	10.1 ± 0.2^{b}
	Root	3.42 ± 0.0^{c}	38.1 ± 0.0^{c}	111.3 ± 0.0^{c}	20.3 ± 0.0^{b}	208.0 ± 0.6^{c}	0.57 ± 0.02^{c}	7.4 ± 0.01^{c}	0.39 ± 0.01^{c}	11.6 ± 0.2^{a}
Treatment	*p* value	< 0.0001	< 0.0001	< 0.0001	< 0.0001	< 0.0001	< 0.0001	< 0.0001	< 0.0001	< 0.0001
Organ	*p* value	< 0.0002	< 0.0001	< 0.0001	< 0.0001	< 0.0001	< 0.0001	< 0.0001	< 0.0001	< 0.0001
T × O	*p* value	< 0.0003	< 0.0001	< 0.0001	< 0.0001	< 0.0001	< 0.0001	< 0.0001	< 0.0001	< 0.0001

Note: Values are means ± standard error ($n = 3$). Different superscript letters indicate significant differences among treatment × organ combinations according to Tukey's HSD test ($p < 0.05$). Statistical significance was determined for treatment, organ, and treatment × organ interaction (T × O) effects.
Abbreviations: APX, ascorbate peroxidase; CAT, catalase; FW, fresh weight; SOD, superoxide dismutase.

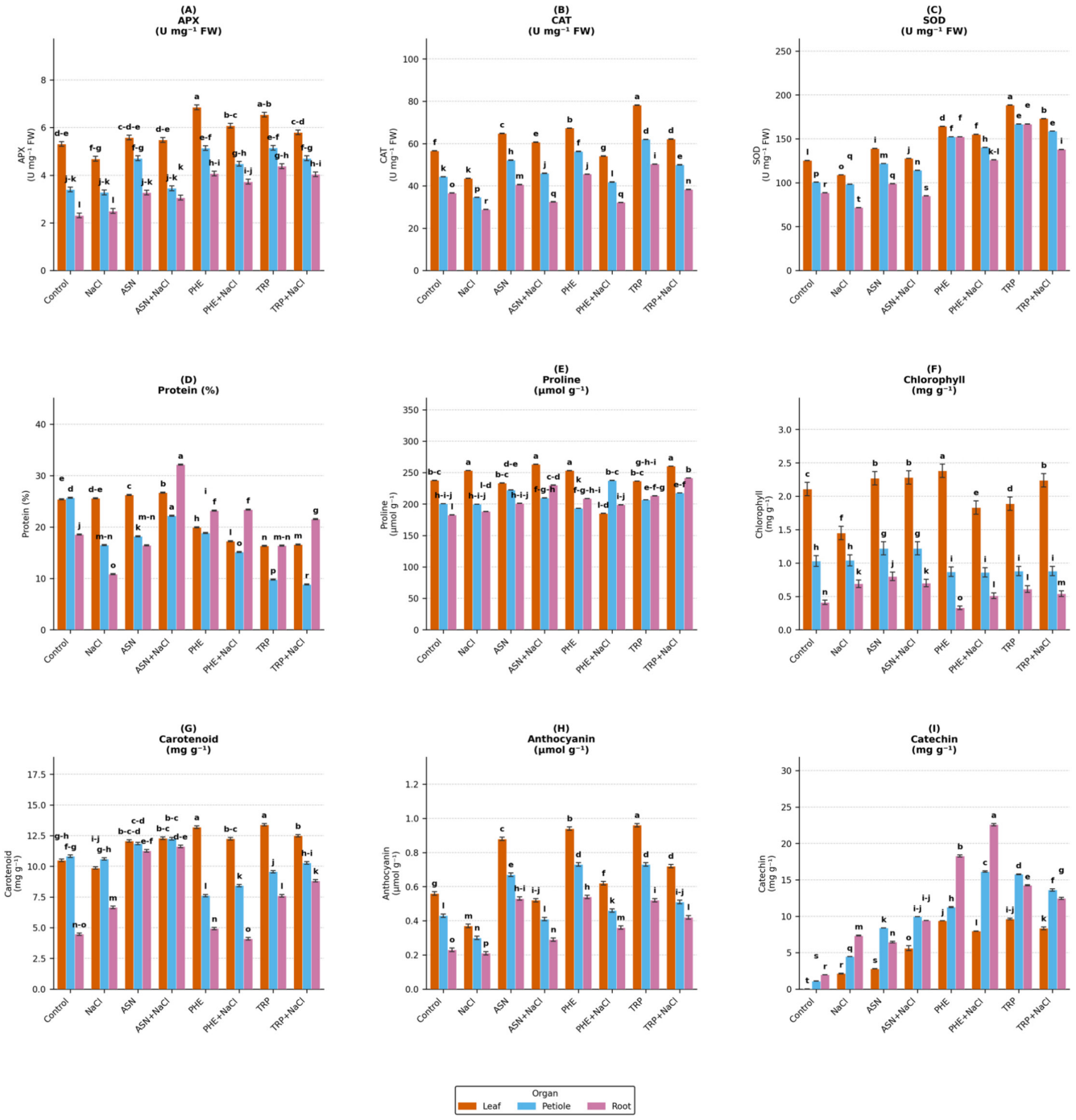

FIGURE 2 | Antioxidant enzyme activities, protein content, osmolyte accumulation, photosynthetic pigments, and secondary metabolite concentrations in leaf, petiole, and root tissues of spinach (*Spinacia oleracea* L.) plants subjected to exogenous amino acid and biostimulant applications under salt stress conditions. Values are means ± SE ($n = 3$). Different lowercase letters above bars indicate significant differences among treatment × organ combinations (Tukey's HSD test, $p < 0.0001$ for treatment, organ, and treatment × organ interaction effects).

3.3 | Amino Acid Effects on Phenolic Compounds and Antioxidant Capacity in Salt-Stressed Spinach

Phenolic acid profiles revealed amino acid-specific modulation of the phenylpropanoid pathway, with all parameters showing significant treatment, organ, and treatment × organ interaction effects ($p < 0.0001$, except dihydroxy benzoic acid organ effect $p = 0.158$, and naringenin organ effect $p = 0.904$ (Table 3 and Figure 3)). Cinnamic acid, the entry-point metabolite of the phenylpropanoid pathway, accumulated to highest levels in phenylalanine and asparagine treatments (PHE: 0.27 mg g^{-1}; ASN: 0.23 mg g^{-1}; ASN + NaCl: 0.24 mg g^{-1}), with PHE and ASN leaves showing 5.4–6.6 fold increases compared to control leaves (0.05 mg g^{-1}), reflecting enhanced phenylalanine ammonia-lyase activity. Caffeic acid demonstrated contrasting accumulation patterns, with asparagine under salinity inducing the highest levels (ASN + NaCl: 0.49 mg g^{-1}), particularly in petioles (0.59 mg g^{-1}) and roots (0.57 mg g^{-1}), representing 8–30 fold

TABLE 3 | Effect of exogenous amino acid applications on individual phenolic acids, flavonoids, total phenolic and flavonoid contents, and antioxidant capacity in leaf, petiole, and root tissues of spinach plants under salt stress conditions.

Applications		Cinnamic acid ($mg g^{-1}$)	Caffeic acid ($mg g^{-1}$)	Dihydroxy benzoic acid ($mg g^{-1}$)	Trans ferulic acid ($mg g^{-1}$)	Rutin trihidrate ($mg g^{-1}$)	Naringenin ($mg g^{-1}$)	Ellagic acid ($mg g^{-1}$)	Quercetine ($mg g^{-1}$)	TPC: total phenolic (mg GAE g^{-1})	TFC: total flavonoid (mg QE g^{-1})	FRAP ($\mu mol g^{-1}$)	PMA (%)
Treatment	Control	0.14 ± 0.01^{e}	0.07 ± 0.03^{g}	0.0037 ± 0.0002^{d}	0.28 ± 0.01^{c}	0.66 ± 0.04^{e}	0.005 ± 0.000^{b}	0.02 ± 0.00^{d}	0.0161 ± 0.0002^{e}	0.80 ± 0.00^{cd}	0.19 ± 0.00^{e}	0.09 ± 0.00^{b}	23.74 ± 4.87^{g}
	NaCl	0.06 ± 0.00^{g}	0.30 ± 0.01^{d}	0.0022 ± 0.0002^{d}	0.34 ± 0.00^{a}	0.10 ± 0.00^{f}	0.007 ± 0.000^{a}	0.01 ± 0.00^{d}	0.0166 ± 0.0002^{e}	0.63 ± 0.05^{e}	0.15 ± 0.01^{f}	0.03 ± 0.00^{de}	17.35 ± 1.44^{h}
	ASN	0.23 ± 0.02^{c}	0.38 ± 0.08^{b}	0.0102 ± 0.0006^{ab}	0.27 ± 0.03^{c}	1.69 ± 0.21^{a}	0.005 ± 0.001^{b}	0.14 ± 0.01^{b}	0.1248 ± 0.0006^{b}	1.06 ± 0.12^{a}	0.24 ± 0.02^{b}	0.02 ± 0.00^{e}	28.99 ± 2.11^{e}
	PHE	0.27 ± 0.00^{a}	0.33 ± 0.11^{c}	0.0117 ± 0.0005^{ab}	0.27 ± 0.02^{c}	0.39 ± 0.00^{d}	0.007 ± 0.000^{a}	0.11 ± 0.01^{b}	0.0493 ± 0.0005^{c}	0.83 ± 0.11^{bc}	0.22 ± 0.01^{c}	0.11 ± 0.01^{a}	39.62 ± 1.12^{a}
	TRP	0.12 ± 0.01^{f}	0.22 ± 0.03^{e}	0.0044 ± 0.0003^{cd}	0.30 ± 0.08^{b}	0.11 ± 0.00^{f}	0.004 ± 0.001^{c}	0.04 ± 0.00^{cd}	0.0232 ± 0.0003^{d}	0.87 ± 0.45^{bc}	0.22 ± 0.11^{c}	0.03 ± 0.01^{de}	36.04 ± 2.45^{b}
	ASN + NaCl	0.24 ± 0.01^{b}	0.49 ± 0.01^{a}	0.0135 ± 0.0007^{a}	0.20 ± 0.01^{f}	1.51 ± 0.22^{b}	0.006 ± 0.000^{ab}	0.24 ± 0.02^{a}	0.1958 ± 0.0007^{a}	1.06 ± 0.08^{a}	0.26 ± 0.03^{a}	0.04 ± 0.01^{c}	25.51 ± 4.11^{f}
	PHE + NaCl	0.18 ± 0.02^{d}	0.31 ± 0.01^{d}	0.0084 ± 0.0004^{bc}	0.23 ± 0.07^{e}	0.24 ± 0.02^{e}	0.004 ± 0.000^{c}	0.06 ± 0.00^{c}	0.0453 ± 0.0004^{c}	0.89 ± 0.12^{b}	0.20 ± 0.11^{de}	0.03 ± 0.01^{d}	30.37 ± 1.11^{c}
	TRP + NaCl	0.03 ± 0.01^{h}	0.19 ± 0.02^{f}	0.0035 ± 0.0003^{d}	0.25 ± 0.01^{d}	0.09 ± 0.00^{f}	0.004 ± 0.000^{c}	0.04 ± 0.00^{cd}	0.0232 ± 0.0003^{d}	0.73 ± 0.00^{d}	0.20 ± 0.02^{d}	0.04 ± 0.00^{c}	29.87 ± 1.12^{d}
Organ	Leaf	0.18 ± 0.01^{a}	0.24 ± 0.00^{c}	0.008 ± 0.001^{a}	0.37 ± 0.01^{a}	0.23 ± 0.03^{c}	0.005 ± 0.001^{a}	0.07 ± 0.05^{b}	0.0474 ± 0.0001^{c}	1.1 ± 0.01^{a}	0.25 ± 0.01^{a}	0.03 ± 0.01^{b}	35.5 ± 0.06^{a}
	Petiole	0.17 ± 0.01^{b}	0.29 ± 0.01^{b}	0.007 ± 0.001^{a}	0.24 ± 0.01^{b}	1.02 ± 0.03^{a}	0.005 ± 0.001^{a}	0.07 ± 0.001^{b}	0.0595 ± 0.0001^{b}	0.8 ± 0.01^{b}	0.21 ± 0.00^{c}	0.08 ± 0.01^{a}	24.0 ± 0.06^{c}
	Root	0.12 ± 0.00^{c}	0.31 ± 0.01^{a}	0.006 ± 0.001^{a}	0.18 ± 0.01^{c}	0.53 ± 0.03^{b}	0.005 ± 0.001^{a}	0.11 ± 0.04^{a}	0.0789 ± 0.0001^{a}	0.7 ± 0.01^{c}	0.23 ± 0.01^{b}	0.03 ± 0.01^{c}	27.3 ± 0.06^{b}
Treatment	*p* value	<0.0001	<0.0001	<0.0001	<0.0001	<0.0001	<0.0001	<0.0001	<0.0001	<0.0001	<0.0001	<0.0001	<0.0001
Organ	*p* value	<0.0001	<0.0001	0.158	<0.0001	<0.0001	0.904	<0.0001	<0.0001	<0.0001	<0.0001	<0.0001	<0.0001
T×O	*p* value	<0.0001	<0.0001	<0.0001	<0.0001	<0.0001	<0.0001	<0.0001	<0.0001	<0.0001	<0.0001	<0.0001	<0.0001

Note: Values are means ± standard error ($n = 3$). Different superscript letters indicate significant differences among treatment × organ combinations according to Tukey's HSD test ($p < 0.05$). Statistical significance was determined for treatment, organ, and treatment × organ interaction (T × O) effects.
Abbreviations: FRAP, ferric reducing antioxidant power; PMA, phosphomolybdate scavenging activity; TFC, total flavonoid content; TPC, total phenolic content.

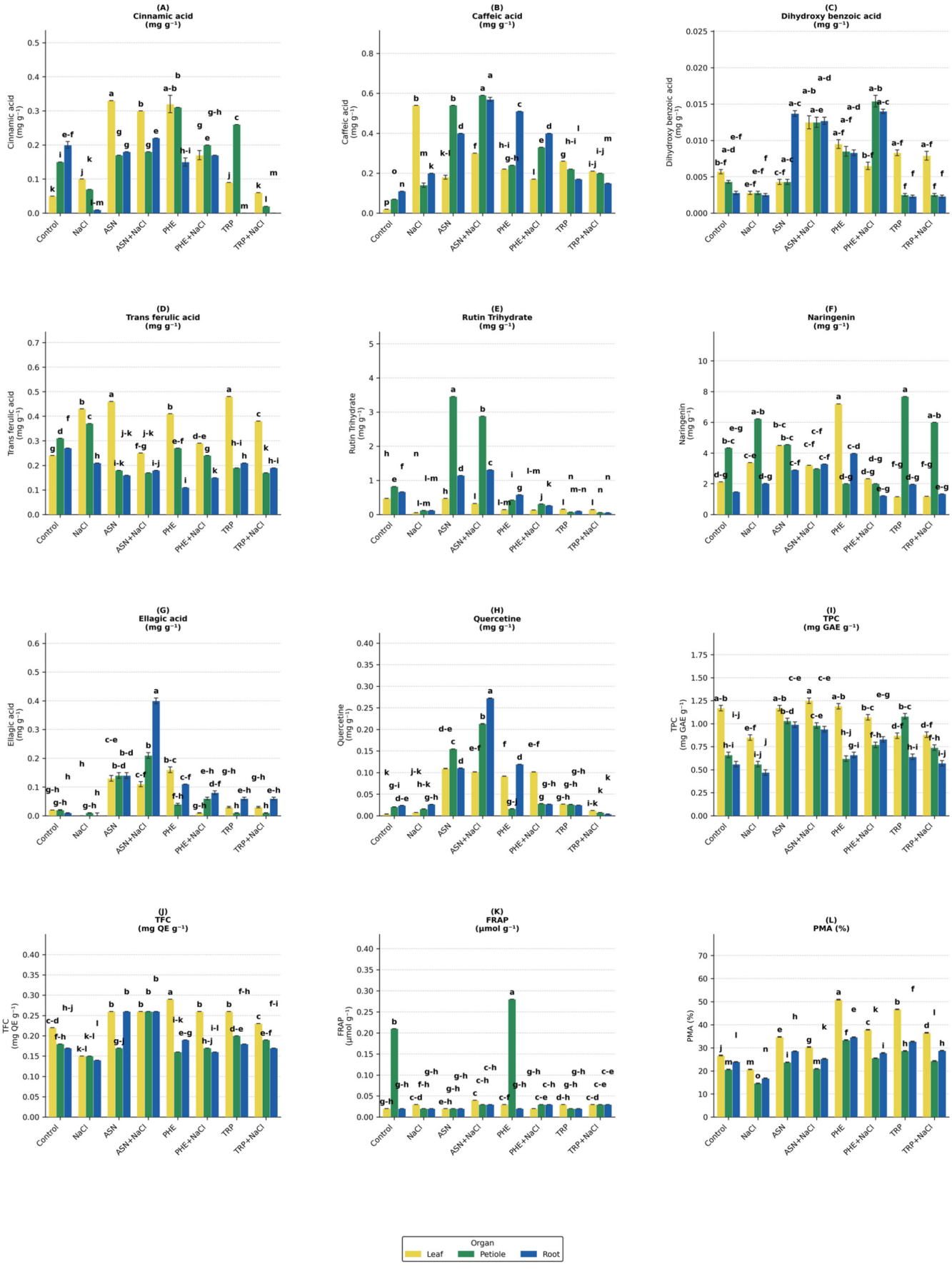

FIGURE 3 | Legend on next page.

FIGURE 3 | Individual phenolic acid profiles, flavonoid composition, total phenolic and flavonoid contents, and antioxidant capacity in leaf, petiole, and root tissues of spinach (*Spinacia oleracea* L.) plants subjected to exogenous amino acid and biostimulant applications under salt stress conditions. Values are means ± SE ($n = 3$). Different lowercase letters above bars indicate significant differences among treatment × organ combinations (Tukey's HSD test, $p < 0.0001$ for treatment, organ, and treatment × organ interaction effects).

increases compared to control leaves. Trans ferulic acid showed stress-induced enhancement, with NaCl treatment achieving the highest accumulation (0.34 mg g^{-1}), though aromatic amino acid leaves also exhibited substantial levels (TRP: 0.48 mg g^{-1}; ASN: 0.46 mg g^{-1}; PHE: 0.41 mg g^{-1}), representing 79%–100% increases compared to control. Dihydroxy benzoic acid accumulated preferentially under ASN + NaCl treatment (0.0135 mg g^{-1}), with 4-5 fold increases across all organs compared to control. Flavonoid profiles demonstrated remarkable amino acid specificity, with asparagine showing unique capacity for quercetin and rutin enhancement. Quercetin content reached maximum levels in ASN + NaCl treatment (0.1958 mg g^{-1}), with roots showing exceptional accumulation (0.2724 mg g^{-1})—an 11-fold increase compared to control roots. Rutin trihydrate exhibited the most dramatic response to asparagine, with ASN treatment achieving 1.69 mg g^{-1} and ASN petioles reaching 3.45 mg g^{-1}, representing a 4.2-fold increase compared to control petioles. Naringenin showed preferential accumulation under aromatic amino acid treatments, with PHE leaves (7.20 mg g^{-1}) and TRP petioles (7.67 mg g^{-1}) exhibiting 3.2–3.6 fold increases. Ellagic acid demonstrated asparagine-salinity synergy, with ASN + NaCl roots showing 40-fold increases (0.40 mg g^{-1}) compared to control roots, indicating activation of specialized polyphenolic biosynthetic pathways.

Total phenolic and flavonoid contents reflected integrated phenylpropanoid pathway activity. Total phenolic content was highest in asparagine treatments (ASN and ASN + NaCl: 1.06 mg g^{-1}), with ASN + NaCl leaves reaching maximum concentration (1.25 mg g^{-1}), while NaCl stress alone resulted in the lowest TPC (0.63 mg GAE g^{-1}). Total flavonoid content showed remarkable uniformity in ASN + NaCl treatment (0.26 mg g^{-1} across all organs), representing 18%–86% increases compared to control tissues, while PHE leaves exhibited maximum TFC (0.29 mg QE g^{-1}). From an organ perspective, leaves consistently maintained the highest TPC (1.1 mg GAE g^{-1}) and TFC (0.25 mg QE g^{-1}), reflecting preferential phenolic accumulation in photosynthetic tissues. Antioxidant capacity assessments revealed tissue-specific and treatment-dependent patterns. Ferric reducing antioxidant power showed exceptional enhancement in phenylalanine-treated petioles (0.28 μmol g^{-1}), representing a 13-fold increase compared to control petioles, indicating vascular tissues serve as major sites for reducing antioxidant accumulation. Phosphomolybdate scavenging activity was highest in aromatic amino acid treatments, with PHE (39.62%) and TRP (36.04%) showing 67%–91% increases compared to control (23.74%), with PHE leaves exhibiting maximum capacity (50.91%). NaCl stress alone resulted in the lowest PMA activity (17.35%), indicating severely impaired antioxidant defense, while amino acid supplementation under salinity substantially restored activity levels. Overall, asparagine demonstrated unique efficacy in stimulating quercetin, rutin, ellagic acid, and caffeic acid biosynthesis, particularly under saline conditions, suggesting activation of specific flavonol and polyphenolic branches of the phenylpropanoid pathway. Phenylalanine excelled in enhancing cinnamic acid, naringenin, and overall antioxidant capacity, reflecting its role as the direct precursor for phenylpropanoid metabolism. Tryptophan showed moderate effects on most phenolic compounds but substantially enhanced trans ferulic acid and naringenin in specific tissues. The pronounced accumulation of diverse phenolic compounds under amino acid treatments, particularly asparagine and phenylalanine, indicates comprehensive activation of secondary metabolism to provide multifaceted antioxidant protection, UV shielding, and stress signaling capacity critical for salt stress tolerance (Table 3 and Figure 3).

3.4 | General Evaluation

The correlation heatmap revealed significant relationships among mineral nutrients, physiological parameters, and secondary metabolites in spinach under amino acid treatments and salt stress (Figure 4). Sodium showed strong negative correlations with anthocyanin (−0.67), TFC (−0.75), PMA (−0.78), and antioxidant enzymes (APX: −0.67, CAT: −0.73, SOD: −0.63), while exhibiting positive correlations with Cl (0.96), K (0.61), and trans ferulic acid (0.64). Chloride displayed similar negative associations with anthocyanin (−0.67), TFC (−0.75), PMA (−0.78), and antioxidant enzymes (APX: −0.65, CAT: −0.82, SOD: −0.58), while exhibiting positive correlations with K (0.43) and trans ferulic acid (0.44). Potassium negatively correlated with carotenoid (−0.73), proline (−0.69), and chlorophyll (−0.70). Antioxidant enzymes showed strong intercorrelations (APX-CAT: 0.81, APX-SOD: 0.94, CAT-SOD: 0.77) and positive associations with photosynthetic pigments and secondary metabolites, indicating coordinated antioxidant defense activation. Phenolic compounds exhibited strong positive correlations among themselves, with quercetin correlating with ellagic acid (0.84), caffeic acid (0.83), and TPC (0.84). Principal component analysis revealed distinct clustering patterns across three metabolic domains (Figure 5). In mineral nutrient space (Figure 5A), Dim1 (40.5%) and Dim2 (32.9%) explained 73.4% of variance. Magnesium, calcium, and phosphorus formed a tight cluster in the negative Dim1 quadrant with high cos2 values (> 0.75), indicating coordinate divalent cation accumulation under TRP + NaCl treatment, while sodium and chloride clustered oppositely in positive Dim1/Dim2. Potassium loaded distinctly in positive Dim1, separating from other nutrients and reflecting its inverse relationship with amino acid supplementation. The Na/K ratio positioned between Na and K vectors.

Physiological parameter analysis (Figure 5B) showed Dim1 (60.9%) and Dim2 (17.5%) explaining 78.4% of variance. Antioxidant enzymes (SOD, CAT, APX) and anthocyanin clustered tightly in negative Dim1/positive Dim2 with high cos2 values (0.8–0.9). Chlorophyll and carotenoid grouped with antioxidant enzymes. Proline positioned distinctly in

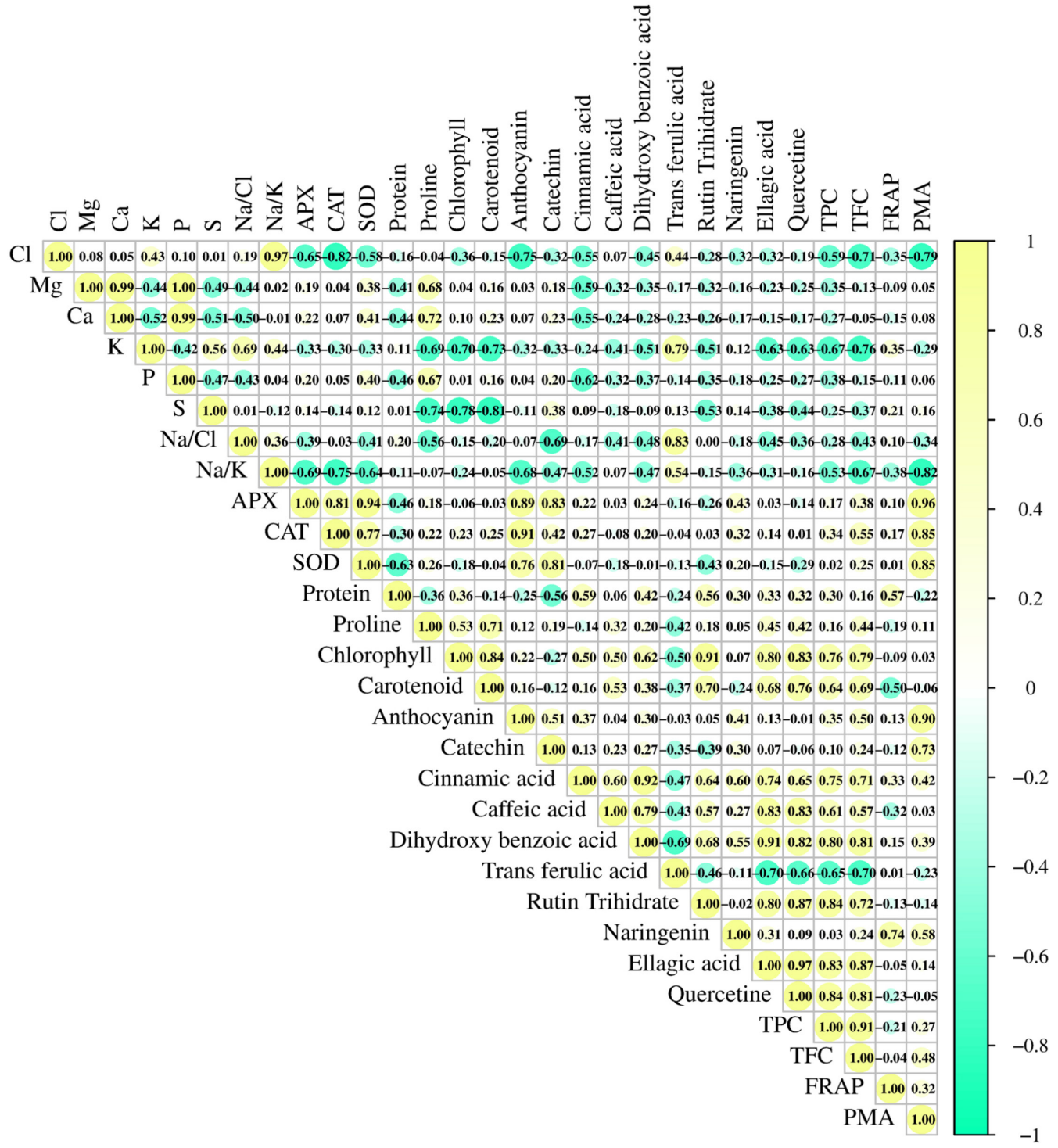

FIGURE 4 | Pearson correlation matrix showing relationships among mineral nutrients, physiological parameters, and secondary metabolites in spinach under amino acid and salt stress treatments. Only correlations with $p < 0.05$ are displayed. APX, ascorbate peroxidase; Ca, calcium; CAT, catalase; Cl, chloride; FRAP, ferric reducing antioxidant power; K, potassium; Mg, magnesium; Na, sodium; Na/Cl, sodium to chloride ratio; Na/K, sodium to potassium ratio; P, phosphorus; PMA, phosphomolybdate scavenging activity; S, sulfur; SOD, superoxide dismutase; TFC, total flavonoid content; TPC, total phenolic content.

negative Dim2 with high cos2, separating from antioxidant systems and reflecting its independent osmolyte function under ASN + NaCl and TRP + NaCl. Protein loaded opposite to anthocyanin, consistent with metabolic trade-offs where tryptophan's secondary metabolism enhancement occurred at protein synthesis expense. Secondary metabolite PCA (Figure 5C) revealed Dim1 (32.3%) and Dim2 (9.8%) explaining 42.1% of variance. Total phenolic and flavonoid contents loaded strongly in positive Dim1 with high cos2 (> 0.8). Quercetin, ellagic acid, caffeic acid, and rutin trihydrate formed a tight cluster in positive Dim1/negative Dim2, reflecting asparagine-specific enhancement of flavonol branches

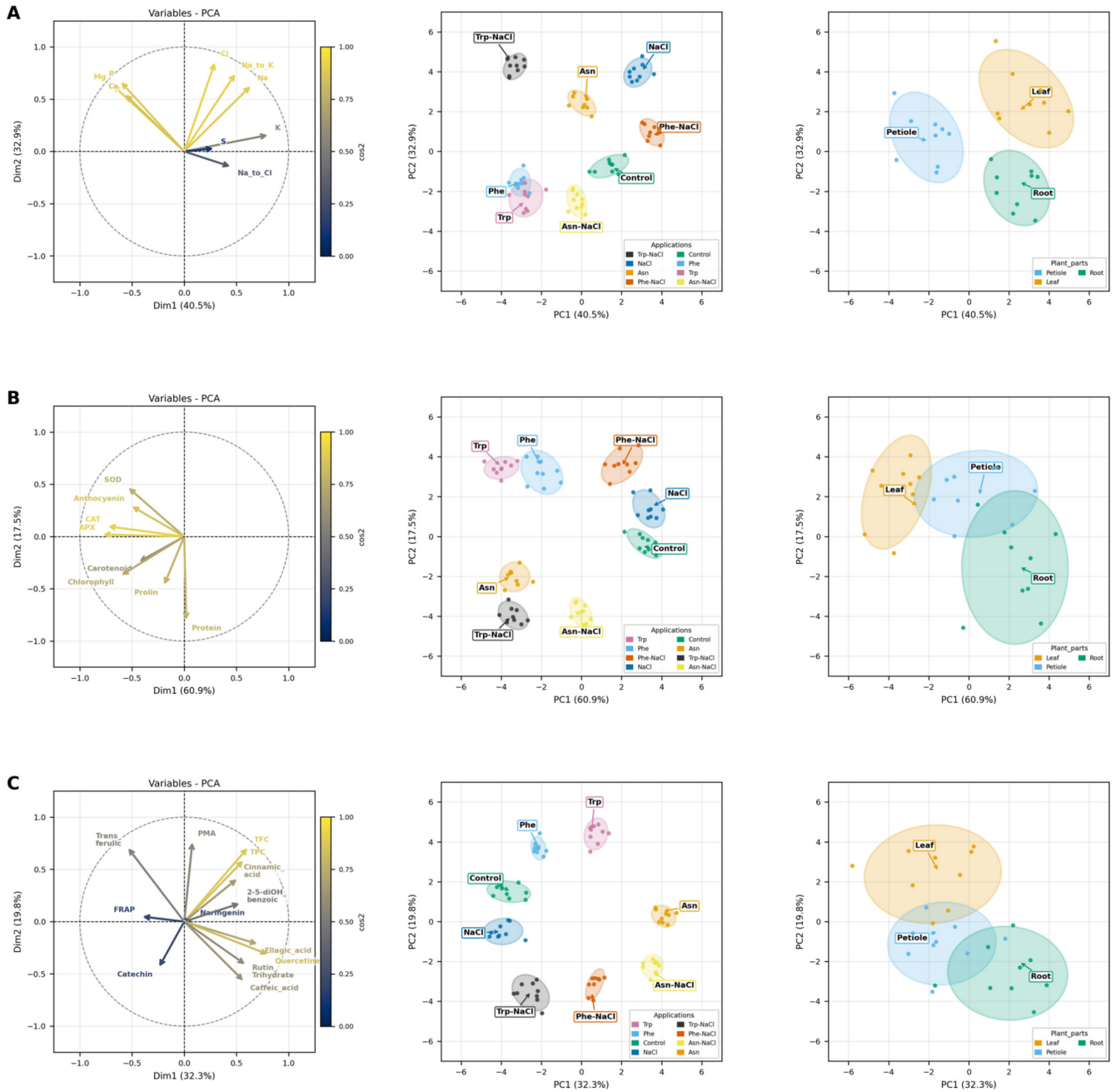

FIGURE 5 | Principal component analysis (PCA) of mineral nutrients (A), physiological parameters (B), and secondary metabolites (C) in spinach under amino acid and salt stress treatments. APX, ascorbate peroxidase; Ca, calcium; CAT, catalase; Cl, chloride; FRAP, ferric reducing antioxidant power; K, potassium; Mg, magnesium; Na, sodium; Na/Cl, sodium to chloride ratio; Na/K, sodium to potassium ratio; P, phosphorus; PMA, phosphomolybdate scavenging activity; S, sulfur; SOD, superoxide dismutase; TFC, total flavonoid content; TPC, total phenolic content.

under salinity. Cinnamic acid and dihydroxy benzoic acid positioned in positive Dim1/Dim2, associated with phenylalanine treatments and representing early pathway intermediates. Trans ferulic acid separated in positive Dim2, reflecting stress-specific induction. Hierarchical clustering analysis revealed distinct metabolic profiles separating treatments and organs (Figure 6). The heatmap showed clear bifurcation between two major clusters: TRP + NaCl treatments (all organs) grouped together with exceptionally high values (green) for Mg, Ca, P, PMA, and CAT. The remaining treatments formed a second major cluster, with amino acid treatments (ASN, PHE, TRP without salt, and their NaCl combinations) separating from control and NaCl-only treatments. Within this cluster, ASN and ASN + NaCl treatments across organs showed elevated values for secondary metabolites including quercetin, caffeic acid, ellagic acid, and rutin trihydrate. NaCl-treated samples clustered separately, characterized by high Na and Cl values (green) but low values (blue) for chlorophyll, carotenoid, and antioxidant enzymes. Control samples formed an intermediate cluster with moderate values across most parameters. Organ-specific clustering patterns emerged, with leaves generally showing higher pigment and phenolic contents, while roots exhibited elevated catechin and quercetin under ASN + NaCl treatment.

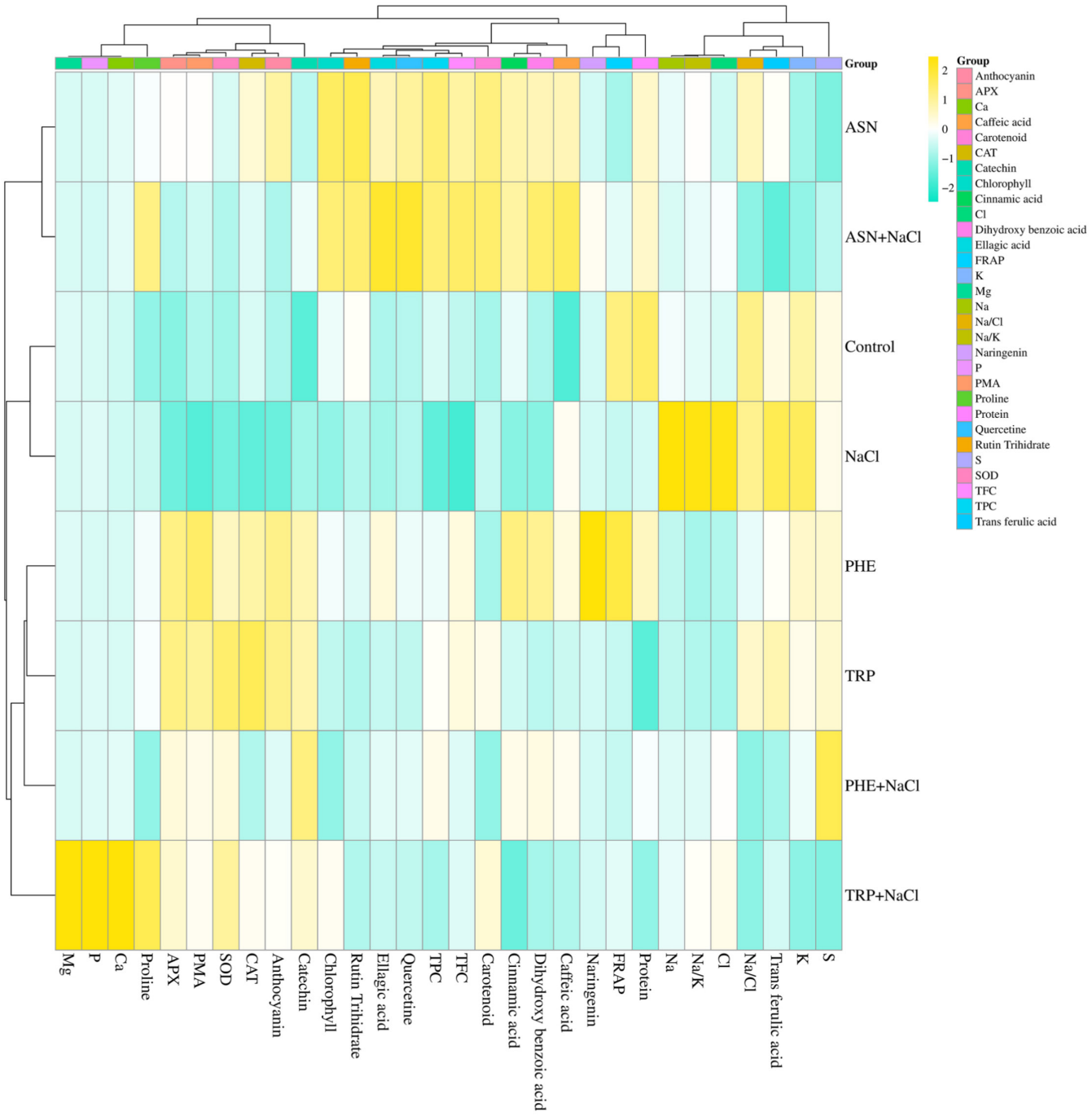

FIGURE 6 | Hierarchical clustering heatmap of all measured parameters across treatment-organ combinations in spinach under amino acid and salt stress conditions. 2,5-dihydroxy benzoic acid, dihydroxy benzoic acid; APX, ascorbate peroxidase; Asn, asparagine; Ca, calcium; CAT, catalase; Cl, chloride; FRAP, ferric reducing antioxidant power; K, potassium; Mg, magnesium; Na, sodium; Na/Cl, sodium to chloride ratio; Na/K, sodium to potassium ratio; P, phosphorus; Phe, phenylalanine; PMA, phosphomolybdate scavenging activity; S, sulfur; SOD, superoxide dismutase; TFC, total flavonoid content; TPC, total phenolic content; Trp, tryptophan.

4 | Discussion

4.1 | Mineral Nutrition and Ionic Homeostasis Under Amino Acid Supplementation

The observed mineral nutrient dynamics and ionic balance alterations in spinach under amino acid supplementation and salt stress conditions provide compelling evidence for the multifaceted roles of exogenous amino acids in modulating plant nutrition and stress tolerance mechanisms. The pronounced accumulation of sodium and chloride under NaCl stress, reaching treatment averages of 6369.9 and 72051.1 mg kg^{-1} respectively (Table 1), reflects the inevitable consequence of salt exposure on ionic homeostasis in glycophytes. However, the remarkable mitigation achieved through amino acid supplementation, particularly the 76% reduction in leaf Na^+ content with asparagine treatment (16346.0 vs. 68861.3 mg kg^{-1}), suggests that these compounds engage sophisticated mechanisms

beyond simple osmotic adjustment. This protective effect likely involves enhanced expression of plasma membrane Na^+/H^+ antiporters and tonoplast-localized ion transporters, enabling more efficient Na^+ compartmentalization into vacuoles and reduced cytoplasmic Na^+ toxicity, as demonstrated by Hasana and Miyake (2017). Similar Na^+ exclusion mechanisms were reported by Abdelkader et al. (2023), who showed that exogenous amino acid applications significantly reduced Na^+ accumulation in lettuce under salt stress, and by Saddique et al. (2022), who demonstrated improved nutrient balance in spinach following amino acid supplementation. The superior performance of phenylalanine in maintaining the lowest sodium treatment average (7208.9 mg kg^{-1}) and its exceptional chloride exclusion capacity aligns with findings by Atteya et al. (2022), who reported that exogenous phenylalanine supplementation enhanced ion selectivity in moringa under salt stress. The differential organ-specific accumulation patterns observed, with leaves accumulating the highest average Na (20585.8 mg kg^{-1}) and Cl (30932.3 mg kg^{-1}), correspond with the observations of Azeem et al. (2023), who demonstrated that Na accumulation was higher in leaves and stems than in roots under saline conditions. The dramatic 3.5-fold increase in Na/K ratio under NaCl stress (2.01 compared to control: 0.58), with roots exhibiting the highest value (2.32), indicates severe disruption of K^+/Na^+ selectivity. The remarkable restoration of ionic balance by all amino acid treatments, ASN + NaCl (0.63), PHE + NaCl (0.57), and TRP + NaCl (0.78), demonstrates their profound impact on ion homeostasis mechanisms, with phenylalanine achieving a 72% reduction in Na/K ratio compared to NaCl alone (Table 1).

The extraordinary accumulation of divalent cations in TRP + NaCl-treated plants represents one of the most striking findings, with treatment averages for Mg, Ca, and P reaching 40414.3, 44743.9, and 15088.0 mg kg^{-1} respectively, representing 6–10 fold increases compared to control plants (Table 1). This coordinate elevation suggests that tryptophan, when combined with salt stress, triggers a unique metabolic reprogramming that fundamentally alters nutrient acquisition priorities. The mechanism underlying this phenomenon may involve tryptophan's role as a precursor to auxin biosynthesis, as noted by Turfan et al. (2024), who demonstrated that TRP acts as a precursor to the root hormone auxin, potentially enhancing root metabolic activity. This auxin-mediated enhancement of root development and mineral uptake capacity is consistent with observations by Goche et al. (2020), who demonstrated that auxin signaling coordinates root architecture modifications that enhance mineral acquisition efficiency under stress conditions. The observation that TRP + NaCl plants simultaneously accumulated exceptional divalent cations while maintaining relatively modest Na^+ levels (14995.4 mg kg^{-1} treatment average) suggests that tryptophan-derived auxin preferentially activates transporters with specificity for divalent over monovalent cations. The preferential enhancement of Ca^{2+} uptake by asparagine supplementation (7372.1 mg kg^{-1}), with petioles showing remarkable accumulation (10436.3 mg kg^{-1}), may be explained by asparagine's dual role as both a nitrogen donor and a signaling molecule, aligning with the work of Guo et al. (2023), who demonstrated that ASN involvement in nitrogen metabolism influences multiple ion transport systems. The observed salt-induced Ca^{2+} deficiency under NaCl stress alone (4235.6 mg kg^{-1}) reflects the well-documented phenomenon of Na^+-Ca^{2+} competition at membrane transport sites, as discussed by Yin et al. (2023). The contrasting potassium nutrition patterns, where NaCl stress induced the highest K^+ accumulation (32229.4 mg kg^{-1}) while amino acid treatments substantially reduced K levels (18980.6 mg kg^{-1}), likely reflect a sophisticated metabolic trade-off prioritizing divalent over monovalent cation acquisition. This preferential regulation may be explained by the differential energetic costs and functional benefits of various cations under stress conditions, as noted by Marium et al. (2021), who described Mg's role in chlorophyll biosynthesis and enzyme activation. The reduction in K^+ accumulation may also reflect improved ionic homeostasis, as demonstrated by Marium et al. (2021), who indicated that exogenous phenylalanine and methionine reverse salinity-induced suppression of essential mineral accumulation. The organ-specific distribution patterns, with leaves maintaining the highest average K (26550.1 mg kg^{-1}), demonstrate preferential allocation to photosynthetic tissues, as emphasized by Sofy et al. (2020).

The sulfur nutrition results, showing highest concentrations in PHE + NaCl treatment (794.9 mg kg^{-1}) with exceptional leaf accumulation (1354.7 mg kg^{-1}), provide important insights into amino acid-mediated enhancement of antioxidant precursor availability. This 66% increase compared to control leaves suggests that phenylalanine promotes sulfate uptake and assimilation under salinity, potentially supporting synthesis of sulfur-containing antioxidants. This finding gains additional significance when considered alongside the work of Guo et al. (2023), who demonstrated that asparagine enhances secondary metabolism by stimulating the synthesis of sulfur-containing amino acids. The enhanced sulfur nutrition under PHE + NaCl aligns with observations by Bakry et al. (2018), who reported that phenylalanine supplementation in flax improved overall mineral acquisition including sulfur-containing compounds. The consistent Na/Cl ratio of 0.48 across all amino acid-salinity combinations, representing a 47% reduction compared to control (0.90), reveals an intriguing aspect of amino acid-mediated ionic regulation that likely involves coordinated regulation of both Na^+ and Cl^- transporters rather than affecting them independently. The contrasting low S levels under asparagine treatments (585 and 626.0 mg kg^{-1}) suggest amino acid-specific differences in sulfur metabolism. The consistent Na/Cl ratio of 0.48 across all amino acid-salinity combinations, representing a 47% reduction compared to control (0.90), reveals an intriguing aspect of amino acid-mediated ionic regulation (Table 1). Overall, the mineral nutrition and ionic balance results demonstrate that exogenous amino acid supplementation represents a sophisticated agronomic intervention that engages multiple levels of plant nutritional physiology, with phenylalanine excelling in maintaining ionic homeostasis and enhanced sulfur nutrition, asparagine effectively excluding toxic ions while promoting calcium uptake, and tryptophan uniquely activating multiple nutrient uptake pathways under salinity.

4.2 | Antioxidant Systems and Secondary Metabolite Dynamics

The antioxidant defense responses and secondary metabolite accumulation patterns observed under amino acid supplementation reveal sophisticated biochemical adaptations that extend

beyond simple osmotic adjustment or ion exclusion mechanisms. The pronounced enhancement of antioxidant enzyme activities, particularly under tryptophan supplementation (CAT: 63.48 U mg^{-1} FW; SOD: 170.29 U mg^{-1} FW), with TRP leaves exhibiting maximum activities representing 23%–50% increases compared to control, demonstrates the capacity of aromatic amino acids to prime enzymatic defense systems (Table 2). This remarkable upregulation likely involves tryptophan-mediated activation of stress-responsive transcription factors that coordinately induce antioxidant gene expression, a phenomenon analogous to the stress priming mechanisms described by Bukhari et al. (2021). The mechanistic basis for tryptophan's superior enzyme activation may lie in its indole ring structure, which can directly function as an antioxidant while simultaneously serving as a precursor for indoleacetic acid (auxin) that upregulates defense gene expression (Turfan et al. 2024). In contrast, phenylalanine demonstrated equivalent APX activity (5.36 U mg^{-1} FW) to TRP while channeling greater metabolic flux into phenylpropanoid pathway-derived antioxidants, suggesting complementary but mechanistically distinct defense activation strategies between these two aromatic amino acids. The severely compromised antioxidant enzyme activities under NaCl stress alone (APX: 3.50; CAT: 35.69; SOD: 93.01 U mg^{-1} FW) reflect the well-documented phenomenon whereby salt stress can paradoxically suppress antioxidant systems while simultaneously generating excessive reactive oxygen species. The substantial recovery of enzyme activities under combined amino acid-salt treatments (TRP + NaCl achieving 36%–68% enhancements compared to NaCl alone) suggests that exogenous amino acids provide both the metabolic precursors necessary for enzyme synthesis and signaling molecules that activate defense gene transcription, aligning with observations of Turfan et al. (2024), who demonstrated TRP's capacity to mitigate harmful effects of salinity on various physiological parameters in spinach. The strong intercorrelations among antioxidant enzymes (APX-CAT: 0.81, APX-SOD: 0.94, CAT-SOD: 0.77) indicate coordinated regulation of these enzymatic systems, consistent with their sequential roles in ROS detoxification (Table 2).

The contrasting protein content patterns present one of the most intriguing findings, revealing fundamental metabolic trade-offs that operate under amino acid supplementation. The dramatic protein reduction under NaCl stress (17.64% average, with roots showing only 10.84%) reflects the severe disruption of nitrogen metabolism and protein synthesis machinery that characterizes salt toxicity, as emphasized by Azeem et al. (2023). However, the remarkable protein concentration in ASN + NaCl roots (32.12%), representing a 196% increase compared to NaCl-stressed roots and a 73% increase even compared to control roots (18.54%), suggests that asparagine supplementation fundamentally reprograms root metabolism under stress conditions, as demonstrated by Akın and Kaya (2024), who showed ASN's capacity to enhance stress resilience in maize through nitrogen metabolism support. Asparagine's unique capacity to enhance root protein accumulation can be explained by its dual role as both a direct substrate for protein synthesis and a mobile nitrogen storage compound that facilitates nitrogen remobilization from amino acid catabolism under stress (Guo et al. 2023). This finding is particularly significant from an agronomic perspective, as roots are critical organs for mineral acquisition and stress sensing, and enhanced root protein content likely reflects greater enzymatic capacity for ion transport and stress signal transduction. Conversely, the lowest protein content observed under TRP and TRP + NaCl treatments (14.16% and 15.65% respectively) reveals the metabolic cost of tryptophan's remarkable enhancement of mineral nutrition and secondary metabolism, aligning with the concept of metabolic resource allocation under stress, as suggested by Jamil et al. (2018), who noted TRP's role in inducing glucosinolate and alkaloid production. The proline accumulation patterns, showing highest levels under amino acid-salinity combinations (TRP + NaCl: 239.89 μmol g^{-1}; ASN + NaCl: 234.37 μmol g^{-1}), representing 13%–16% increases compared to control, confirm the well-established role of this osmolyte in stress tolerance (Table 2). The organ-specific accumulation, with leaves showing the highest average proline (240.4 μmol g^{-1}), suggests functional compartmentalization where osmotic adjustment is prioritized in photosynthetically active tissues, aligning with findings by Wang et al. (2022), who identified higher proline content in watermelon leaves subjected to drought stress. The differential effects of amino acids on proline accumulation, with all three amino acids enhancing proline under both stressed and unstressed conditions, as reported by Almas et al. (2021) in tomato with PHE, Guo et al. (2023) in Methylocytsi with ASN, and Turfan et al. (2024) in spinach with TRP, suggest that these compounds activate proline biosynthetic pathways through multiple mechanisms.

The photosynthetic pigment responses reveal amino acid-specific protective effects that directly preserve photosynthetic capacity under salt stress. Asparagine's maintenance of the highest chlorophyll levels (1.43 mg g^{-1}), with ASN + NaCl effectively protecting against salt-induced degradation (1.40 vs. 1.07 mg g^{-1} in NaCl alone, representing 31% enhancement), suggests that this amino acid either promotes chlorophyll biosynthesis or inhibits chlorophyll degradation by chlorophyllase enzymes. This chlorophyll-protective effect of asparagine is consistent with its role in maintaining nitrogen pools available for chlorophyll biosynthesis, as the porphyrin ring of chlorophyll is nitrogen-rich and requires sustained nitrogen supply for both synthesis and repair (Kaya et al. 2013). The carotenoid enhancement under aromatic amino acid treatments (TRP and PHE leaves showing 22%–28% increases compared to control) reflects activation of the carotenoid biosynthetic pathway, with these photoprotective pigments serving critical roles in dissipating excess light energy and scavenging singlet oxygen under stress conditions, as emphasized by Wilson et al. (2021). The catechin response represents perhaps the most dramatic secondary metabolite enhancement, with PHE + NaCl inducing the highest accumulation (15.56 mg g^{-1}), particularly in roots (22.58 mg g^{-1}), representing a 10-fold increase compared to control roots. This preferential root accumulation of catechins aligns with observations by Zhang et al. (2017) and Savina et al. (2023), who emphasized roots' role as storage organs for phenolic compounds crucial for defense against soil-borne pathogens and heavy metal stress.

4.3 | Phenolic Profiles and Antioxidant Capacity Modulation

The phenolic compound profiles and antioxidant capacity measurements reveal the biochemical culmination of amino

acid-mediated metabolic reprogramming, demonstrating how these exogenous supplements fundamentally reshape secondary metabolism to enhance stress defense capabilities. The remarkable enhancement of cinnamic acid, the gateway metabolite of the phenylpropanoid pathway, under phenylalanine and asparagine treatments provides direct evidence for enhanced phenylalanine ammonia-lyase activity, as noted by Atteya et al. (2022), who emphasized PHE's role in promoting biosynthesis of cinnamic acid and related compounds. This enzyme catalyzes the deamination of phenylalanine to cinnamic acid, representing the committed step that channels primary metabolites into secondary metabolism. The substantial elevation of this entry-point metabolite under phenylalanine supplementation confirms that substrate availability limits phenylpropanoid pathway flux under normal conditions, and that exogenous phenylalanine relieves this bottleneck, enabling enhanced production of downstream defensive compounds. The contrasting accumulation pattern of caffeic acid, showing highest levels under asparagine-salinity combination, particularly in petioles and roots, reveals pathway-specific regulation that differs fundamentally from the early phenylpropanoid steps, as proposed by Guo et al. (2023), who demonstrated ASN's involvement in modulating multiple metabolic pathways through nitrogen metabolism enhancement. The preferential accumulation in petioles and roots, rather than in leaves where cinnamic acid predominantly accumulates, suggests tissue-specific regulation of hydroxylation capacity and potentially differential transport of hydroxylated versus non-hydroxylated phenolic acids, aligning with findings by Feduraev et al. (2019), who identified distinct phenolic compound distributions across organs including predominance of benzoic acid, cinnamic acid, quercetin, and catechin with highest concentrations in petioles near roots. The stress-induced enhancement of trans ferulic acid indicates that this particular hydroxycinnamic acid responds strongly to stress signals independently of amino acid supplementation, consistent with its established role in cell wall cross-linking and lignification responses to stress where plants strengthen their physical barriers against environmental challenges.

The flavonoid profiles reveal remarkable substrate and pathway specificity that clearly differentiates amino acid effects on secondary metabolism. The extraordinary quercetin accumulation in asparagine-salinity treatment, with roots showing an 11-fold increase compared to controls, demonstrates asparagine's unique capacity to activate the flavonol branch of flavonoid biosynthesis (Table 3). The mechanism by which asparagine, a non-aromatic amino acid that does not directly enter the phenylpropanoid pathway, achieves such dramatic activation of flavonol biosynthesis likely involves indirect effects through enhanced nitrogen metabolism and the availability of carbon skeletons for phenylpropanoid precursors, as proposed by Guo et al. (2023). Furthermore, asparagine may enhance the expression of key flavonol biosynthesis genes including flavonoid 3′-hydroxylase and flavonol synthase through its role in nitrogen signaling networks. The rutin trihydrate response represents the most dramatic organ-specific flavonoid accumulation, with ASN petioles reaching 3.45 $mg\,g^{-1}$, a 4.2-fold increase over control petioles, suggesting rutin may serve specialized vascular protection functions. The ellagic acid accumulation showing 40-fold increases in ASN + NaCl roots compared to control, as documented also by Savina et al. (2023), represents activation of specialized polyphenolic biosynthetic pathways. An interesting contrast emerges regarding anthocyanin distribution: the present results showing highest anthocyanin in aromatic amino acid treatments differ somewhat from Feduraev et al. (2019), who reported anthocyanin highest in leaves of Rumex species, and from Savina et al. (2023), who observed highest anthocyanin in roots of meadowsweet. These discrepancies likely reflect species-specific differences in anthocyanin regulation, developmental stage effects, and the specific amino acid treatments applied, emphasizing that organ-specific anthocyanin accumulation patterns are not universal but depend on the experimental system and stress conditions.

The total phenolic content results, showing highest levels in asparagine treatments, provide an integrative measure demonstrating that asparagine broadly activates phenylpropanoid metabolism rather than enhancing only specific branch pathways (Table 3). The dramatic contrast with salt stress alone, resulting in the lowest total phenolic content, confirms that salt stress per se suppresses overall phenolic biosynthesis, likely through disruption of primary metabolism that provides precursors and energy for secondary metabolism, as noted by Sarker and Oba (2019) and Zhang et al. (2017). The organ-specific distribution, with leaves maintaining highest total phenolic content, reflects the particular importance of phenolic compounds in protecting photosynthetic tissues where light-induced reactive oxygen species generation creates intense oxidative pressure, as emphasized by Savina et al. (2023), who documented organ-specific antioxidant capacity patterns with highest levels in leaves reflecting their primary role in photosynthesis and metabolic activity. The total flavonoid content showing remarkable uniformity in asparagine-salinity treatment across all organs demonstrates comprehensive activation of flavonoid biosynthesis throughout the plant. This distribution aligns with observations by Feduraev et al. (2019) and Liu et al. (2022), who documented that total flavonoid content was primarily localized in leaves, though interesting discrepancies exist regarding specific compound distributions. The modulation of secondary metabolite activity by tryptophan may be attributed to its role in inducing glucosinolate and alkaloid production, as noted by Jamil et al. (2018), whereas phenylalanine exerts its effect by promoting biosynthesis of cinnamic acid, anthocyanins, and flavonoids, as demonstrated by Atteya et al. (2022) and Almas et al. (2021). In contrast, asparagine enhances secondary metabolism by stimulating synthesis of sulfur-containing amino acids, which are key precursors in biosynthesis of secondary metabolites, as shown by Guo et al. (2023). The antioxidant capacity measurements, assessed through multiple assays, reveal that the highest ferric reducing antioxidant power activity was recorded in roots under phenylalanine treatments, whereas phosphomolybdenum assay exhibited greatest values in leaves with phenylalanine and tryptophan supplements, supporting the interpretation that aromatic amino acids serve as key precursors in secondary metabolic pathways, as noted by Zhu et al. (2017), while asparagine functions primarily as a donor of carbon and nitrogen, as demonstrated by Kaya et al. (2013). Overall, the phenolic compound and antioxidant capacity results demonstrate that amino acid supplementation, particularly asparagine, fundamentally restructures secondary metabolism with organ-specific specialization reflecting distinct physiological roles, where leaves serve as primary sites of photosynthesis requiring

high defense against stressors, while roots function as storage organs for metabolites and phenolic compounds crucial for defense against soil microorganisms, as emphasized by Zhang et al. (2017) and Savina et al. (2023).

5 | Conclusion

Our study revealed that amino acid selection significantly influences spinach resilience to salt stress through distinct metabolic reprogramming pathways. Each amino acid demonstrated unique protective mechanisms across mineral nutrition, antioxidant defense, and secondary metabolism. Phenylalanine excelled in maintaining ionic homeostasis, achieving the lowest sodium treatment average and superior Na/K ratio restoration, while enhancing phenylpropanoid pathway activation through elevated cinnamic acid biosynthesis. Asparagine demonstrated remarkable specificity in excluding toxic ions while promoting calcium uptake and uniquely enhancing root protein accumulation under salinity, alongside comprehensive activation of flavonol branches evidenced by dramatic quercetin, rutin, and ellagic acid accumulation. Tryptophan triggered the most striking metabolic reprogramming, inducing exceptional divalent cation accumulation representing 6–10-fold increases while maximally enhancing antioxidant enzyme activities, though at the cost of reduced protein synthesis. Organ-specific patterns revealed leaves as primary sites for photosynthetic pigments and phenolic compounds, roots as storage organs for specialized flavonoids and catechins, and petioles exhibiting exceptional rutin accumulation. Based on these findings, asparagine is recommended for comprehensive metabolic defense and photosynthetic capacity maintenance, phenylalanine for ionic exclusion and antioxidant enhancement, and tryptophan where mineral nutrition improvement is the priority. Future research should focus on field validation across varying salinity levels, optimization of application timing and concentration, and examination of synergistic effects when combining multiple amino acids.

Author Contributions

N.T. contributed to conceptualization, investigation, resources, supervision, and led the writing of the original draft and its review and editing. O.K. contributed to conceptualization, investigation, methodology, and writing – review and editing. K.T. was responsible for data curation, investigation, software, visualization. E.M.A. contributed to data curation, formal analysis. F.Y. participated in investigation, methodology, and validation.

Acknowledgements

The authors express their sincere gratitude to the Kastamonu University Scientific Research Coordination Unit for financial support provided through project number KÜBAP-10/23-20, which enabled the chemical analyses conducted in this study. Also, generative AI tools were used exclusively for linguistic editing and language refinement of this manuscript. No AI-generated scientific content, data analysis, or interpretation was produced. All scientific contributions, data, and conclusions are solely the responsibility of the authors.

Funding

This work was supported by Kastamonu University Scientific Research Coordination Unit (KÜBAP-10/23-20).

Conflicts of Interest

The authors declare no conflicts of interest.

Data Availability Statement

The datasets generated and analyzed during the current study are available from the corresponding author upon reasonable request.

References

Abdelkader, M., L. Voronina, O. Shelepova, et al. 2023. "Monitoring Role of Exogenous Amino Acids on the Proteinogenic and Ionic Responses of Lettuce Plants Under Salinity Stress Conditions." *Horticulturae* 9, no. 6: 626. https://doi.org/10.3390/horticulturae9060626.

Aebi, H. 1984. "Catalase In Vitro." In *Methods in Enzymology*, vol. 105, 121–126. Academic press.

Akın, S., and C. Kaya. 2024. "Asparagine and Nitric Oxide Jointly Enhance Antioxidant Capacity and Nitrogen Metabolism to Improve Drought Resistance in Cotton: Evidence From Long-Term Field Trials." *Food and Energy Security* 13: e502. https://doi.org/10.1002/fes3.502.

Almas, H. I., Z. un-Nisa, and S. Anwar. 2021. "Exogenous Application of Methionine and Phenylalanine Confers Salinity Tolerance in Tomato by Concerted Regulation of Metabolites and Antioxidants." *Journal of Soil Science and Plant Nutrition* 21: 3051–3064. https://doi.org/10.1007/s42729-021-00588-9.

Atteya, A. K. G., R. S. El-Serafy, K. M. El-Zabalawy, A. Elhakem, and E. A. E. Genaidy. 2022. "Exogenously Supplemented Proline and Phenylalanine Improve Growth, Productivity, and Oil Composition of Salted Moringa by Up-Regulating Osmoprotectants and Stimulating Antioxidant Machinery." *Plants* 11, no. 12: 1553. https://doi.org/10.3390/plants11121553.

Azeem, M., K. Pirjan, M. Qasim, A. Mahmood, T. Javed, and H. Muhmmad. 2023. "Salinity Stress Improves Antioxidant Potential by Modulating Physio-Biochemical Responses in *Moringa oleifera* Lam." *Scientific Reports* 13, no. 1: 2895.

Bakhoum, G. S., E. A. E. Badr, M. S. Sadak, O. M. Kabesh, and G. A. Ain. 2019. "Improving Growth, Some Biochemical Aspects and Yield of Three Cultivars of Soybean Plant by Methionine Treatment Under Sandy Soil Condition." *International Journal of Environmental Research* 13, no. 1: 35–43. https://doi.org/10.1007/s41742-018-0148-1.

Bakry, A. B., H. M. S. El-Bassiouny, M. S. Sadak, and A. S. M. Younis. 2018. "Yield, Quantity and Quality of Two Flax Cultivars Affected by Phenylalanine and Methionine Under Sandy Soil Conditions." *Bioscience Research* 5, no. 4: 3838–3854.

Bates, L. S., R. P. Waldern, and I. D. Teare. 1973. "Rapid Determination of Free Proline for Water-Stress Studies." *Plant and Soil* 39: 205–207.

Beauchamp, C., and I. Fridovich. 1971. "Superoxide Dismutase: Improved Assays and an Assay Applicable to Acrylamide Gels." *Analytical Biochemistry* 44, no. 1: 276–287.

Benzie, I. F. F., and J. J. Strain. 1996. "The Ferric Reducing Ability of Plasma (FRAP) as a Measure of 'Antioxidant' Power: The FRAP Assay." *Analytical Biochemistry* 239: 70–76.

Bradstreet, R. B. 1954. "Kjeldahl Method for Organic Nitrogen." *Analytical Chemistry* 26, no. 1: 185–187.

Bukhari, M. A., M. S. Sharif, Z. Ahmad, et al. 2021. "Silicon Mitigates the Adverse Effect of Drought in canola (Brassica napus L.) through Promoting the Physiological and Antioxidants Activity." *Silicon* 13, no. 11: 3817–3826.

Chouaibi, M. 2025. "Bioactive Phytochemicals From Spinach (*Spinacia oleracea* L.) By-Products." In *Bioactive Phytochemicals in By-Products From Leaf, Stem, Root and Tuber Vegetables*, edited by M. F. Ramadan. Springer. https://doi.org/10.1007/978-3-031-80700-8_5.

El-Awadi, M. E., M. S. Sadak, M. A. Khater, and M. G. Dawood. 2025. "Melatonin Stimulates Salt Tolerance of Soybean Plants by Modulating Photosynthetic Performance, Osmoregulation, and the Enzymatic Antioxidant Defence System." *Acta Biologica Slovenica* 8, no. 3: 120–141. https://doi.org/10.14720/abs.68.3.21635.

El-Lethy, S. R., M. S. Sadak, and R. S. Hanafy. 2024. "Assessing the Usefulness of *Moringa oleifera* Leaf Extract and Zeatin in Enhancing Growth, Phytohormones, Antioxidant Enzymes and Osmoprotectants of Wheat Plant Under Salinity Stress." *Egyptian Journal of Botany* 64, no. 3: 183–196. https://doi.org/10.21608/ejbo.2024.252447.2587.

FAO. 2024. "Food and Agriculture Organisation of the United Nations." https://www.fao.org/faostat/en/#home.

Feduraev, P., G. Chupakhina, P. Maslennikov, N. Tacenko, and L. Skrypnik. 2019. "Variation in Phenolic Compounds Content and Antioxidant Activity of Different Plant Organs From *Rumex crispus* L. and *Rumex obtusifolius* L. at Different Growth Stages." *Antioxidants* 8, no. 7: 237. https://doi.org/10.3390/antiox8070237.

Feduraev, P., L. Skrypnik, A. Riabova, et al. 2020. "Phenylalanine and Tyrosine as Exogenous Precursors of Wheat (*Triticum aestivum* L.) Secondary Metabolism Through PAL-Associated Pathways." *Plants* 9, no. 4: 476. https://doi.org/10.3390/plants9040476.

Goche, T., N. G. Shargie, I. Cummins, A. P. Brown, S. Chivasa, and R. Ngara. 2020. "Comparative Physiological and Root Proteome Analyses of Two Sorghum Varieties Responding to Water Limitation." *Scientific Reports* 10, no. 1: 11835. https://doi.org/10.1038/s41598-020-68735-3.

Guo, K., T. Glatter, N. Paczia, and W. Liesack. 2023. "Asparagine Uptake: A Cellular Strategy of *Methylocystis* to Combat Severe Salt Stress." *Applied and Environmental Microbiology* 89, no. 6: e0011323. https://doi.org/10.1128/aem.00113-23.

Hasana, R., and H. Miyake. 2017. "Salinity Stress Alters Nutrient Uptake and Causes Damage of Root and Leaf Anatomy in Maize." *KnE Life Sciences* 3, no. 4: 219. https://doi.org/10.18502/KLS.V3I4.708.

Hussain, M., H. Fatima, A. Khan, A. Ghani, and M. Nadeem. 2018. "Improving Salinity Tolerance in Brassica (*Brassica napus* Var. Bsa and *Brassica campestris* Var. Toria) by Exogenous Application of Proline and Glycine Betaine." *Biological Sciences* 61: 1–8.

Jamil, M., M. A. Kharal, M. Ahmad, et al. 2018. "Inducing Salinity Tolerance in Red Pepper (*Capsicum annuum* L.) Through Exogenous Application of Proline and L-Tryptophan." *Soil and Environment* 37, no. 2: 160–168. https://doi.org/10.25252/SE/18/31052.

Kaya, C., S. Aydemir, O. Sonmez, M. Ashraf, and M. Dikilitas. 2013. "Regulation of Growth and Some Key Physiological Processes in Salt-Stressed Maize (*Zea mays* L.) Plants by Exogenous Application of Asparagine and Glycerol." *Acta Botanica Croatica* 72, no. 1: 57–168.

Khan, A., H. Fatima, A. Ghania, et al. 2018. "Improving Salinity Tolerance in Brassica (*Brassica napus* Var. Bsa and *Brassica campestris* Var. Toria) by Exogenous Application of Proline and Glycine." *Pakistan Journal of Scientific and Industrial Research Series B, Biological Sciences* 61, no. 1: 1–8. https://doi.org/10.52763/PJSIR.BIOL.SCI.61.1.2018.1.8.

Khattab, H. I., M. S. Sadak, M. G. Dawood, F. M. A. Elkady, and N. M. Helal. 2024. "Foliar Application of Esculin and Digitoxin Improve the Yield Quality of Salt-Stressed Flax by Improving the Antioxidant Defense System." *BMC Plant Biology* 24, no. 1: 963. https://doi.org/10.1186/s12870-024-05626-z.

Kim, B. M., H. J. Lee, Y. H. Song, and H. J. Kim. 2021. "Effect of Salt Stress on the Growth, Mineral Contents, and Metabolite Profiles of Spinach." *Journal of the Science of Food and Agriculture* 101, no. 9: 3787–3794. https://doi.org/10.1002/jsfa.11011.

Kumaran, A., and R. J. Karunakaran. 2006. "Nitric Oxide Radical Scavenging Active Components From *Phyllanthus emblica* L." *Plant Foods for Human Nutrition* 61, no. 1: 1–5.

Lichtenthaler, H. K. 1987. "Chlorophylls and Carotenoids: Pigments of Photosynthetic Biomembranes." In *Methods in Enzymology*, vol. 148, 350–382. Academic Press.

Liu, W., Z. Zhang, T. Zhang, Q. Qiao, and X. Hou. 2022. "Phenolic Profiles and Antioxidant Activity in Different Organs of *Sinopodophyllum hexandrum*." *Frontiers in Plant Science* 13: 1037582. https://doi.org/10.3389/fpls.2022.1037582.

Liu, X., S. Chen, F. Du, et al. 2023. "Insights Into Adaptive Regulation of the Leaf-Root System: Strategies for Survival of Water Lily Plants Under Salt Stress." *International Journal of Molecular Sciences* 24: 5605. https://doi.org/10.3390/ijms24065605.

Mancinelli, A. L. 1990. "Interaction Between Light Quality and Light Quantity in the Photoregulation of Anthocyanin Production." *Plant Physiology* 92, no. 4: 1191–1195.

Marium, A., A. Kausar, M. Y. Ashraf, H. Kanwal, and Z. I. H. Nazli. 2021. "Enhancement in Biomass and Nutrient Uptake in Cucumber Through Methionine and Phenylalanine Under Saline Soils." *Pakistan Journal of Agricultural Sciences* 58, no. 1: 125–134. https://doi.org/10.21162/PAKJAS/21.10014.

Nakano, Y., and K. Asada. 1981. "Hydrogen Peroxide Is Scavenged by Ascorbate-Specific Peroxidase in Spinach Chloroplasts." *Plant and Cell Physiology* 22, no. 5: 867–880.

Prieto, P., M. Pineda, and M. Aguilar. 1999. "Spectrophotometric Quantitation of Antioxidant Capacity Through the Formation of a Phosphomolybdenum Complex: Specific Application to the Determination of Vitamin E." *Analytical Biochemistry* 269, no. 2: 337–341.

Rodrıguez-Delgado, M. A., S. Malovana, J. P. Perez, T. Borges, and F. G. Montelongo. 2001. "Separation of Phenolic Compounds by High-Performance Liquid Chromatography With Absorbance and Fluorimetric Detection." *Journal of Chromatography A* 912, no. 2: 249–257.

Sadak, M. S., M. T. Abdelhamid, and U. Schmidhalter. 2015. "Effect of Foliar Application of Aminoacids on Plant Yield and Some Physiological Parameters in Faba Bean Plants Irrigated With Seawater." *Acta Biologica Colombiana* 20, no. 1: 141–152.

Sadak, M. S., M. G. Dawood, and M. E. S. El-Awadi. 2024. "Changes in Growth, Photosynthetic Pigments and Antioxidant System of *Hordeum vulgare* Plant Grown Under Salinity Stress via Signal Molecules Application." *Vegetos* 37: 1966–1982. https://doi.org/10.1007/s42535-024-00879-3.

Sadak, M. S., M. E. El-Awadi, M. G. Dawood, and K. G. A. El-Rokiek. 2025. "Role of Phenyalanine as Elicitor to Promote Some Physiological and Biochemical Attributes of Two Wheat Cultivars Grown Under Sandy Soil Conditions." *Agricultural Engineering International* 27, no. 2: 238–248. http://www.cigrjournal.org.

Saddique, M., A. Kausar, I. Iqra, et al. 2022. "Amino Acids Application Alleviated Salinity Stress in Spinach (*Spinacia oleracea* L.) by Improving Oxidative Defence, Osmolyte Accumulation, and Nutrient Balance." *Turkish Journal of Agriculture and Forestry* 46, no. 6: 875–887. https://doi.org/10.55730/1300-011X.3049.

Sarker, U., and S. Oba. 2019. "Salinity Stress Enhances Colour Parameters, Bioactive Leaf Pigments, Vitamins, Polyphenols, Flavonoids and Antioxidant Activity in Selected Amaranthus Leafy Vegetables." *Journal of the Science of Food and Agriculture* 99: 2275–2284. https://doi.org/10.1002/jsfa.9423.

Savina, T., V. Lisun, P. Feduraev, and L. Skrypnik. 2023. "Variation in Phenolic Compounds, Antioxidant and Antibacterial Activities of Extracts From Different Plant Organs of Meadowsweet (*Filipendula ulmaria* (L.) Maxim.)." *Molecules* 28, no. 8: 3512. https://doi.org/10.3390/molecules28083512.

Singleton, V. L., and J. A. Rossi. 1965. "Colorimetry of Total Phenolics With Phosphomolybdic-Phosphotungstic Acid Reagents." *American Journal of Enology and Viticulture* 16: 144–158.

Sofy, M. R., N. Elhawat, and T. Alshaal. 2020. "Glycine Betaine Counters Salinity Stress by Maintaining High K^+/Na^+ Ratio and Antioxidant Defense via Limiting Na^+ Uptake in Common Bean (*Phaseolus vulgaris* L.)." *Ecotoxicology and Environmental Safety* 200: 110732.

Turfan, N. 2023. "The Effects of Exogenous Tyrosine Supplement on Spinach (*Spinacia oleracea* L.) Cultivation Under Lithium Stress." *Mediterranean Agricultural Sciences* 36, no. 3: 101–108. https://doi.org/10.29136/mediterranean.1300307.

Turfan, N. 2025. "Investigation of the Effects of Foliar Amino Acid, Melatonin and Potassium Applications on Spinach Cultivar Under Water Stress." *Bursa Uludag Üniversitesi Ziraat Fakültesi Dergisi* 39: 1–23.

Turfan, N., B. Kibar, N. Davletova, and H. Kibar. 2024. "Ameliorative Effects of Humic Acid and L-Tryptophan on Enzyme Activity, Mineral Content, Biochemical Properties, and Plant Growth of Spinach Cultivated in Saline Conditions." *Food Science & Nutrition* 12: 8324–8339. https://doi.org/10.1002/fsn3.4435.

TURKSTAT. 2024. *Turkish Agricultural Production Statistics*. Turkish Statistical Institute. https://www.tuik.gov.tr/Home/Index.

Wang, Z., Y. Yang, V. Yadav, et al. 2022. "Drought-Induced Proline Is Mainly Synthesized in Leaves and Transported to Roots in Watermelon Under Water Deficit." *Horticultural Plant Journal* 8, no. 5: 615–626.

Wilson, L. M., S. Tharmarajah, Y. Jia, R. D. Semba, D. A. Schaumberg, and K. A. Robinson. 2021. "The Effect of Lutein/Zeaxanthin Intake on Human Macular Pigment Optical Density: A Systematic Review and Meta-Analysis." *Advances in Nutrition* 12, no. 6: 2244–2254.

Yin, Y., S. Fan, and S. Li. 2023. "Involvement of Cell Cycle and Ion Transferring in the Salt Stress Responses of Alfalfa Varieties at Different Development Stages." *BMC Plant Biology* 23: 343. https://doi.org/10.1186/s12870-023-04335-3.

Zhang, P., M. Senge, and Y. Dai. 2017. "Effects of Salinity Stress at Different Growth Stages on Tomato Growth, Yield, and Water-Use Efficiency." *Communications in Soil Science and Plant Analysis* 48, no. 6: 624–634. https://doi.org/10.1080/00103624.2016.1269803.

Zhu, H., X. Li, W. Zhai, et al. 2017. "Effects of Low Light on Photosynthetic Properties, Antioxidant Enzyme Activity, and Anthocyanin Accumulation in Purple Pak-Choi (*Brassica campestris* Ssp. *Chinensis* Makino)." *PLoS One* 12: e0179305.